Stem Cell Reports, Volume *6*

Supplemental Information

Oncometabolic Nuclear Reprogramming of Cancer Stemness

Javier A. Menendez, Bruna Corominas-Faja, Elisabet Cuyàs, María G. García, Salvador Fernández-Arroyo, Agustín F. Fernández, Jorge Joven, Mario F. Fraga, and Tomás Alarcón

Supplemental data

Model formulation

Our model is based on a minimal gene regulatory network, which enables us to study the oncometabolic nuclear reprogramming of differentiated cells into pluripotent stem cells. This network considers the interactions between a minimal core of stemness-associated transcription factors (*OCT4* and *SOX2*) and two generic lineage-specific genes, referred to as *LSG1* and *LSG2*. The model schematically represented in **Fig. 1A** (*top panel*) is similar to a number of previous approaches (Cinquin and Demongeot, 2005; Cinquin and Page, 2007; MacArthur and Lemischka, 2013; MacArthur et al., 2008; Shu et al., 2013), particularly the one considered by Shu et al. (2013), which involves a coupled pluripotency module (i.e., self-activation of *OCT4* and *SOX2*) and a differentiation module (i.e., mutual antagonism between the *LSGs*). However, the model presented here originally introduces the epigenetic regulation of the *LSGs*, which is the essential element that enables us to account for the regulatory effects of certain metabolic features (i.e., oncometabolites) in the nuclear reprogramming process.

Our stochastic model of oncometabolic nuclear reprogramming is formulated in terms of a continuous-time Markov process governed by the corresponding master equation **[1]**, which determines the temporal evolution of the probability density function $P(X,t)$ for the random variable $X(t)$.

$$\frac{\partial P(X,t)}{\partial t} = \sum_{i=1}^{R} \left(W_i(X - r_i) P(X - r_i, t) - W_i(X) P(X,t) \right) \quad \textbf{[1]}$$

X is a random vector whose components correspond to the number of cell states present in our system at time t. $X(t)$ is therefore the state vector of the network whose components are the number of each element involved in the dynamics of the nuclear reprogramming gene network (i.e., the number of molecules of each transcription factor, the number of available binding sites left in the promoter of each gene, and the number of binding sites bound to each of three transcription factor dimers: OCT4-SOX2, LSG1-LSG1, and LSG2-LSG2). R is the number of reactions or events that the system can undergo, also referred to as channels. $W_i(X)$ is the transition rate corresponding to channel i (i.e., the probability that the event associated with the channel i occurs in the time interval $(t,t+\Delta t)$ is $W_i(X(t))\Delta t$ for $\Delta t \rightarrow 0$), and r_i is the change in the state vector X when channel i fires up. In mathematical terms, the probability that $X(t+\Delta t) = X(t) + r_i$ conditioned to the system to be in state $X(t)$ at time t is given by $P(X(t+\Delta t) = X(t) + r_i \,|\, X(t)) = W_i(X(t)\Delta t$.

In other words, the quantities $W_i(X)$ and r_i are, respectively, the transition rates and the state vector change associated with the occurrence of the elementary reaction i. For each gene in the reprogramming network, our stochastic model considers the following set of elementary

reactions: (i) reversible binding of transcription factor dimers to free binding sites in the promoter region, (ii) uninduced protein synthesis, (iii) protein degradation. For the stemness-related transcription factors specifically, we consider a fourth elementary process, namely induced protein synthesis, whereby OCT4 and SOX2 proteins are synthesised independently of the binding of the OCT4-SOX2 heterodimer to their promoters. A detailed description and model of the different processes involved in our stochastic model of oncometabolic nuclear reprogramming follows.

1. Model of the gene regulatory network

Models of gene regulatory networks controlling cell differentiation have generally been studied in terms of mean-field (i.e., deterministic) high-dimensional switches, particularly in the context of competitive heterodimerisation networks (Cinquin and Demongeot, 2005; Cinquin and Page, 2007). Instead, our stochastic model of oncometabolic nuclear reprogramming is based on premises regarding transcription factor binding to gene promoters that have been proposed by the MacArthur's group (MacArthur and Lemischka, 2013; MacArthur et al., 2008).

As mentioned above, our stochastic model considers the pluripotency genes *OCT4* and *SOX2* and two lineage-specific genes (*LSGs*). The stemness-associated transcription factors OCT4 and SOX2 upregulate each other and downregulate the expression of the *LSGs*. The OCT4 and SOX2 protein products form a dimer that binds to the gene promoters of the network; when the OCT4-SOX2 dimer binds to the promoters of *OCT4* and *SOX2*, the OCT4-SOX2 dimer upregulates the expression of *OCT4* and *SOX2*. If, by contrast, the OCT4-SOX2 dimer binds to the promoters of *LSGs*, the OCT4-SOX2 dimer downregulates the expression of *LSGs*. Our model also considers the induction of the expression of *OCT4* and *SOX2* independently of the binding of OCT4-SOX2 dimers to their promoter regions, which makes it possible to model the original Yamanaka mechanism (Takahashi and Yamanaka, 2006; Takahashi et al., 2007), where reprogramming is achieved by transfection with retroviruses encoding the RNA of *OCT4* and *SOX2*.

The stoichiometric equations for the processes involved in the regulation of the *OCT4* promoter region are as follows:

- Reversible binding of dimers to free binding sites in the promoter region of *OCT4*:

$$F_O + O + S \leftrightarrow B_{O,O-S}$$
$$F_O + L_1 + L_1 \leftrightarrow B_{O,1-1}$$
$$F_O + L_2 + L_2 \leftrightarrow B_{O,2-2} \qquad \textbf{[2]}$$

- Uninduced protein synthesis of OCT4:

$$B_{O,O-S} \rightarrow O \qquad \textbf{[3]}$$

- Degradation of the OCT4 protein:

$$O \rightarrow \varnothing \qquad \textbf{[4]}$$

- Induced synthesis of the OCT4 protein:

$$\varnothing \rightarrow O \qquad \textbf{[5]}$$

Similarly, the stoichiometric equations for the processes involved in the regulation of the *SOX2* promoter region are as follows:

- Reversible binding of dimers to free binding sites in the promoter region of *SOX2*:

$$F_S + O + S \leftrightarrow B_{S,O-S}$$
$$F_S + L_1 + L_1 \leftrightarrow B_{S,1-1}$$
$$F_S + L_2 + L_2 \leftrightarrow B_{S,2-2} \qquad \textbf{[6]}$$

- Uninduced protein synthesis of SOX2:

$$B_{S,O-S} \rightarrow S \qquad \textbf{[7]}$$

- Degradation of the SOX2 protein:

$$S \rightarrow \varnothing \qquad \textbf{[8]}$$

- Induced synthesis of the SOX2 protein:

$$\varnothing \rightarrow S \qquad \textbf{[9]}$$

Each of the LSGs self-upregulate and downregulate the expression of the other LSGs as well as of the stemness transcription factors OCT4 and SOX2. The protein products of the LSGs form homodimers (LSG1-LSG1 and LSG2-LSG2) and heterodimers (LSG1-LSG2) that bind to the gene promoters; when the LSG homodimers binds the corresponding promoter, it self-upregulates the expression of the corresponding *LSG*. If the LSG homodimer binds to the promoter of the other *LSG*, the LSG homodimer downregulates the expression of the other *LSG*. The LSG heterodimer always represses the expression of the corresponding *LSG*, regardless of which promoter it binds to. All the possible LSG dimers repress the expression of the stemness factors. The stoichiometric equations corresponding to the dynamics of the LSGs are as follows:

- Reversible binding of dimers to free binding sites in the promoter regions of *LSGs*:

$$F_i + O + S \leftrightarrow B_{i,O-S}$$
$$F_i + L_1 + L_1 \leftrightarrow B_{i,1-1}$$
$$F_i + L_2 + L_2 \leftrightarrow B_{i,2-2} \qquad \textbf{[10]}$$

- Synthesis of LSG proteins:

$$B_{i,O-S} \rightarrow L_i \qquad \textbf{[11]}$$

- Degradation of LSG proteins

$$L_i \rightarrow \varnothing \qquad \textbf{[12]}$$

where $i = 1, 2$.

The details of how we model the dynamics produced by these stoichiometric reactions and, more importantly, how the models for gene and epigenetic regulation are coupled follow.

1.1. Activation and downregulation of transcription: Competitive inhibition. Here, we provide details of how we model the stoichiometric processes **[2]**, **[6]** and **[10]**. Regulation of transcription is achieved using a model where the transcription factors of each gene in the minimal regulatory network compete for the binding sites in their promoter regions (**Fig. 1A**, *bottom panel*). Upon dimerisation, the protein products of the stemness-related transcription factors *OCT4* and *SOX2* and of each *LSG* bind to the promoter region of the different genes in the network. Dimers of OCT4-SOX2 proteins that bind to the promoter regions of *OCT4* and *SOX2* upregulate their transcription, whereas dimers made out of combinations of LSGs repress the transcription of *OCT4* and *SOX2*. Similarly, LSG homodimers (LSG1-LSG1 and LSG2-LSG2) bound to the promoters of the corresponding *LSGs* promote their self-expression. By contrast, binding of any other dimer represses the expression of *LSGs*.

To model the processes of binding and unbinding, we used the standard law of mass action kinetics (Gillespie, 1976). We made two simplifying assumptions, which we argue should have solely minor quantitative effects without altering the qualitative properties of the system. First, we did not explicitly consider the transcription factor dimerisation process. Instead, we assumed that the whole process of dimerisation and dimer binding to the corresponding promoter region can be subsumed under ternary reactions. Thus, under the usual fast kinetics assumption for the formation of the dimer, when the dimer and its components are assumed to be in equilibrium (MacArthur et al., 2008), this approximation should have only minor effects. Second, we did not consider the formation of LSG1-LSG2 heterodimers. The

resulting transition rates are given in **Tables S1**, **S2** and **S3** for the promoter regions of *OCT4*, *SOX2* and the *LSGs*, respectively.

Table S1

Transition rate	ΔO	ΔS	ΔF_O	$\Delta B_{O,O-S}$	$\Delta B_{O,1-1}$	$\Delta B_{O,2-2}$	Description
$W_{11} = k_{11} O S F_O$	-1	-1	-1	+1	0	0	*O*-*S* binding
$W_{12} = k_{12} B_{O,O-S}$	+1	+1	+1	-1	0	0	*O*-*S* unbinding
Transition rate	ΔL_1	ΔL_2	ΔF_O	$\Delta B_{O,O-S}$	$\Delta B_{O,1-1}$	$\Delta B_{O,2-2}$	
$W_{13} = k_{13} L_1 (L_1 - 1) F_O$	-2	0	-1	0	+1	0	L_1 dimer binding
$W_{14} = k_{14} B_{O,1-1}$	+2	0	+1	0	-1	0	L_1 dimer unbinding
$W_{15} = k_{15} L_2 (L_2 - 1) F_O$	0	-2	-1	0	0	+1	L_2 dimer binding
$W_{16} = k_{16} B_{O,2-2}$	0	+2	+1	0	0	-1	L_2 dimer unbinding

Transition rates corresponding to the stochastic model of competitive transcription factor binding to the promoter region of Oct4 (Equation [2]). *O*, *S*, L_1 and L_2 refer to the numbers of OCT4, SOX2, LSG1 and LSG2 proteins. $B_{O,O-S}$, $B_{O,1-1}$ and $B_{O,2-2}$ are the numbers of sites in the promoter region of *OCT4* bound to OCT4-SOX2 dimers, LSG1 dimers and LSG2 dimers, respectively. F_O is the number of free (i.e., unbound) sites in the *OCT4* promoter. ΔO, ΔS, ΔL_1, ΔL_2, ΔF_O, $\Delta B_{O,O-S}$, $\Delta B_{O,1-1}$ and $\Delta B_{O,2-2}$ are the components of the state change vector corresponding to each channel. The remaining components of the state change vector have not been explicitly stated in this table, as they do not affect these reactions and are identically zero.

Table S2

Transition rate	ΔO	ΔS	ΔF_S	$\Delta B_{S,O-S}$	$\Delta B_{S,1-1}$	$\Delta B_{S,2-2}$	Description
$W_{17} = k_{17} O S F_S$	-1	-1	-1	+1	0	0	*O*-*S* Binding
$W_{18} = k_{18} B_{S,O-S}$	+1	+1	+1	-1	0	0	*O*-*S* Unbinding
Transition rate	ΔL_1	ΔL_2	ΔF_S	$\Delta B_{S,O-S}$	$\Delta B_{S,1-1}$	$\Delta B_{S,2-2}$	
$W_{19} = k_{19} L_1 (L_1 - 1) F_S$	-2	0	-1	0	+1	0	L_1 dimer binding
$W_{20} = k_{20} B_{S,1-1}$	+2	0	+1	0	-1	0	L_1 dimer unbinding
$W_{21} = k_{21} L_2 (L_2 - 1) F_S$	0	-2	-1	0	0	+1	L_2 dimer binding
$W_{22} = k_{22} B_{S,2-2}$	0	+2	+1	0	0	-1	L_2 dimer unbinding

Transition rates corresponding to the stochastic model of competitive transcription factor binding to the promoter region of Oct4 (Equation [6]). *O*, *S*, L_1 and L_2 refer to the

numbers of OCT4, SOX2, LSG1 and LSG2 proteins. $B_{S,O-S}$, $B_{S,1-1}$ and $B_{S,2-2}$ are the numbers of sites in the promoter region of *SOX2* bound to OCT4-SOX2 dimers, LSG1 dimers and LSG2 dimers, respectively. F_S is the number of free (i.e., unbound) sites in the *OCT4* promoter. ΔO, ΔS, ΔL_1, ΔL_2, ΔF_O, $\Delta B_{S,O-S}$, $\Delta B_{S,1-1}$ and $\Delta B_{S,2-2}$ are the components of the state change vector corresponding to each channel. The remaining components of the state change vector have not been explicitly stated in this table, as they do not affect these reactions and are identically zero.

Table S3

Transition rate	ΔO	ΔS	ΔF_i	$\Delta B_{i,O-S}$	$\Delta B_{i,1-1}$	$\Delta B_{i,2-2}$	Description
$W_{23+6(i-1)} = k_{23+6(i-1)} OSF_i$	-1	-1	-1	+1	0	0	*O*-*S* binding
$W_{24+6(i-1)} = k_{24+6(i-1)} B_{i,O-S}$	+1	+1	+1	-1	0	0	*O*-*S* unbinding
Transition rate	ΔL_1	ΔL_2	ΔF_i	$\Delta B_{i,O-S}$	$\Delta B_{i,1-1}$	$\Delta B_{i,2-2}$	
$W_{25+6(i-1)} = k_{25+6(i-1)} L_1 (L_1 - 1) F_i$	-2	0	-1	0	+1	0	L_1 dimer binding
$W_{26+6(i-1)} = k_{26+6(i-1)} B_{i,1-1}$	+2	0	+1	0	-1	0	L_1 dimer unbinding
$W_{27+6(i-1)} = k_{27+6(i-1)} L_2 (L_2 - 1) F_i$	0	-2	-1	0	0	+1	L_2 dimer binding
$W_{28+6(i-1)} = k_{28+6(i-1)} B_{i,2-2}$	0	+2	+1	0	0	-1	L_2 dimer unbinding

Transition rates corresponding to the stochastic model of competitive transcription factor binding to the promoter region of the LSGs (Equation [10]). *O*, *S*, L_1 and L_2 refer to the numbers of OCT4, SOX2, LSG1 and LSG2 proteins. $B_{i,O-S}$, $B_{i,1-1}$ and $B_{i,2-2}$ are the numbers of sites in the promoter region of the *LSGs* bound to OCT4-SOX2 dimers, LSG1 dimers and LSG2 dimers, respectively. F_i is the number of free (i.e., unbound) sites in the *LSGs* promoters. ΔO, ΔS, ΔL_1, ΔL_2, ΔF_i, $\Delta B_{i,O-S}$, $\Delta B_{i,1-1}$ and $\Delta B_{i,2-2}$ are the components of the state change vector corresponding to each channel. The remaining components of the state change vector have not been explicitly stated in this table, as they do not affect these reactions and are identically zero. The index i (i = 1,2) spans the set of the different LSGs considered.

The reactions **[2]**, **[6]**, and **[10]**, whose transition rates are given in **Tables S1**, **S2**, and **S3**, respectively, are such that the total number of binding sites within the promoter region of each gene must be conserved, i.e., the following balance equations must be satisfied:

$$F_O + B_{O,O-S} + B_{O,1-1} + B_{O,2-2} = T_O \qquad \textbf{[13]}$$

$$F_S + B_{S,O-S} + B_{S,1-1} + B_{S,2-2} = T_S \qquad \textbf{[14]}$$

$$F_1 + B_{1,O-S} + B_{1,1-1} + B_{1,2-2} = T_1(A_1) \qquad \textbf{[15]}$$

$$F_2 + B_{2,O-S} + B_{2,1-1} + B_{2,2-2} = T_2(A_2) \qquad \textbf{[16]}$$

The above equations, particularly **[15]** and **[16]**, are of crucial relevance for the formulation of our stochastic model, as they incorporate the coupling between genetic and epigenetic regulation. Specifically, we consider that the *LSGs* are under epigenetic regulation and that the number of binding sites within the promoter regions of *LSGs* that are accessible to transcription factors at every given time, T_1 and T_2, are determined by the acetylation status. As a first approximation, we consider the case where $T_1 = C_1A_1$ and $T_2 = C_2A_2$, where C_1 and C_2 are constant. By contrast, we consider the case where T_O and T_S are constant. The process of introducing the model for protein synthesis and degradation is described in **section 1.2** (see below).

1.2. Uninduced and induced protein synthesis and degradation. We proceed further by introducing the model for protein synthesis and degradation. We should first consider the stoichiometric processes described by equations **[3]**, **[4**] and **[5]**, which include protein synthesis and degradation of OCT4. The equation **[3]** describes the uninduced protein synthesis of OCT4. Because the transcription of *OCT4* is upregulated by the binding of OCT4-SOX2 dimers to the free sites within the *OCT4* promoter, we model the synthesis of the OCT4 protein by assuming that its probability rate is proportional to the number of OCT4-SOX2-bound sites ($B_{O,O-S}$). It is relevant to note that uninduced synthesis of OCT4 requires the presence of OCT4 protein, i.e., in the absence of OCT4 protein, $B_{O,O-S} = 0$, and consequently, no synthesis of OCT4 occurs. By contrast, the induced synthesis of OCT4 occurs at a constant rate, R_1, independently of $B_{O,O-S}$, which means that there is a positive probability of induced synthesis of OCT4 at all times. These two processes give rise to a global rate of OCT4 synthesis given by $W_1 = k_1B_{O,O-S} + R_1$ (see **Table S4**). The degradation process is modelled by the standard first-order decay kinetics (as shown in the W_2-entry of **Table S4**). The principles for SOX2 synthesis and degradation are exactly the same as for OCT4. The dynamics of LSG synthesis and degradation are also determined by the same kinetics, except that we do not consider induced synthesis for the LSGs.

Table S4

Transition rate	ΔO	ΔS	ΔL_1	ΔL_2	Description
$W_1 = k_1B_{O,O-S} + R_1$	+1	0	0	0	Oct4 synthesis
$W_2 = k_2O$	-1	0	0	0	Oct4 degradation
$W_3 = k_3B_{S,O-S} + R_1$	0	+1	0	0	Sox2 synthesis
$W_4 = k_4S$	0	-1	0	0	Sox2 degradation
$W_5 = k_5B_{1,1-1}$	0	0	+1	0	LSG1 synthesis
$W_6 = k_6L_1$	0	0	-1	0	LSG1 degradation

$W_7 = k_7 B_{2,2-2}$	0	0	0	+1	LSG2 synthesis
$W_8 = k_8 L_2$	0	0	0	-1	LSG2 degradation

Transition rates corresponding to the stochastic model of competitive transcription factor binding to the promoter region of the LSGs (Equation [10]). O, S, L_1 and L_2 refer to the numbers of OCT4, SOX2, LSG1 and LSG2 proteins. $B_{i,O-S}$, $B_{i,1-1}$ and $B_{i,2-2}$ are the numbers of sites in the promoter region of the *LSGs* bound to OCT4-SOX2 dimers, LSG1 dimers and LSG2 dimers, respectively. F_i is the number of free (i.e., unbound) sites in the *LSGs* promoters. ΔO, ΔS, ΔL_1 and ΔL_2 are the components of the state change vector corresponding to each channel. The remaining components of the state change vector have not been explicitly stated in this table, as they do not affect these reactions and are identically zero.

2. Epigenetic regulation of the lineage-specific genes (LSGs)

Our stochastic model of oncometabolic nuclear reprogramming is a generalisation of the epigenetic model proposed by Dodd et al. (2007), which considers nucleosome modification as the basic mechanism for epigenetic cell memory. Nucleosomes are assumed to be in one of three states, namely methylated (*M*), unmodified (*U*) and acetylated (*A*), and the dynamics of the model is given in terms of the transition rates between the *M*, *U*, and *A* nucleosome states.

As originally postulated by Dodd et al. (2007), our model considers direct transitions between *M* and *A* to be highly unlikely. Instead, our models assume that transitions occur in a linear sequence [**17**] in which *M* nucleosomes can only undergo loss of the corresponding methyl group to become *U* nucleosomes, which can then, through the intervention of the corresponding histone-modifying enzyme, acquire an acetyl group to become *A* nucleosomes, and vice versa.

$$M_i \leftrightarrow U_i \leftrightarrow A_i \qquad \textbf{[17]}$$

The subindex *i* in **[17]** spans the set of LSGs considered (in the current model $i = 1, 2$).

Nucleosome modifications are of two types, namely recruited and unrecruited. A recruited modification refers to a positive feedback mechanism where change in the modification status of the nucleosome is facilitated by the presence of other modified nucleosomes (*i.e.,* by the presence of other methylated or acetylated nucleosomes). Mathematically, a recruited modification is expressed through a non-linear dependence on the number of *M*-nucleosomes and *A*-nucleosomes of the corresponding transition rates (see **Table S5**). An unrecruited modification refers to nucleosome modifications whose probability is independent of the modification status of the other nucleosomes. The corresponding transition rates are given in **Table S5**.

Table S5

Transition rate	ΔM_i	ΔU_i	ΔA_i	Description
$W_{35+8(i-1)} = k_{35+8(i-1)} h_2 M_i A_i$	-1	+1	0	Recruited nucleosome demethylation
$W_{36+8(i-1)} = k_{36+8(i-1)} h_1 M_i U_i$	+1	-1	0	Recruited nucleosome methylation
$W_{37+8(i-1)} = k_{37+8(i-1)} h_4 M_i A_i$	0	+1	-1	Recruited nucleosome deacetylation
$W_{38+8(i-1)} = k_{38+8(i-1)} h_3 M_i U_i$	0	-1	+1	Recruited nucleosome acetylation
$W_{39+8(i-1)} = k_{39+8(i-1)} M_i$	-1	+1	0	Unrecruited nucleosome demethylation
$W_{41+8(i-1)} = k_{41+8(i-1)} h_1 U_i$	+1	-1	0	Unrecruited nucleosome methylation
$W_{40+8(i-1)} = k_{40+8(i-1)} A_i$	0	+1	-1	Unrecruited nucleosome deacetylation
$W_{42+8(i-1)} = k_{42+8(i-1)} h_3 U_i$	0	-1	+1	Unrecruited nucleosome acetylation

Transition rates corresponding to the stochastic model of epigenetic regulation. M_i, U_i and A_i with i=1,2 are the number of methylated, unmodified, and acetylated nucleosomes corresponding to the LSG i. ΔM_i, ΔU_i and ΔA_i are the components of the state change vector corresponding to each reaction channel. The remaining components of the state change vector have not been explicitly stated in this table, as they do not affect these reactions and are identically zero.

We added an additional element to the model by Dodd et al. (2007). Nucleosome modifications are mediated by four types of enzymes, namely histone methyltransferases (HMT) and histone acetyl transferases (HAT), which mediate methylation and acetylation, and histone demethylases (HDM) and histone deacetylases (HDAC), which catalyse demethylation and deacetylation. The activities of HAT, HMT, HDM and HDAC are accounted for by the parameters h_1, h_3, h_2 and h_4, respectively (see **Table S5**). These enzymes play a pivotal role in our stochastic model of oncometabolic nuclear reprogramming, as their activity status is the coupling effector between a given metabolic feature (i.e., oncometabolites) and the regulatory differentiation/reprogramming system. In particular, we considered the metabolo-epigenetic connection originally proposed by Thompson's group (Lu and Thompson, 2012; Lu et al., 2012). They were pioneers in showing that, whereas the wild-type form of the IDH enzymes helps cell differentiation to proceed normally by providing HDMs with the corresponding cofactors, the activity of the mutant form of the IDH enzyme drastically hinders HDM activity. The wild-type IDH enzyme catalyses the interconversion of isocitrate and alpha-ketoglutarate (αKG) in cytosol or mitochondria, whereas the neomorphic activity of the mutant form of IDH produces the oncometabolite 2HG from αKG. As the differentiation process is regulated by αKG-dependent HDMs, such as JHDM, the oncometabolite 2HG effectively reduces HDM activity to lock *IDH* mutated-cells in a state poised for the acquisition of pluripotency.

We postulated that our stochastic model should be able to simulate how oncometabolite-induced reduction of HDM, along with the activation of reprogramming stimuli (i.e., the stemness-related transcription factors *OCT4* and *SOX2*), actually leads to a significant increase in the speed and efficiency of the nuclear reprogramming phenomenon.

Supplemental experimental procedures

A. The stochastic model

We employed two different techniques to analyse the diverse aspects of our stochastic model of oncometabolic nuclear reprogramming, namely, direct numerical simulation using Gillespie's stochastic simulation algorithm (SSA) (see **section A. 1**) and the semiclassical approximation (see **section A. 2**). Gillespie's SSA was utilised to study the kinetics of the reprogramming process, whereas the semiclassical approximation enabled us to explore issues such as the enlargement of the basin of attraction of the stemness state upon oncometabolic reduction of HDM activity.

A. 1. Gillespie's stochastic simulation algorithm. Gillespie's SSA is a numerical simulation technique that enables us to generate exact sample paths whose probability density is the solution of the master equation **[1]**. The SSA is a standard technique in the simulation of Markov stochastic processes, and therefore we will not provide a full description here. In short, the algorithm is based on a reformulation of the process described by the master equation, whereby its evolution is driven by the iteration of the following two steps: (i) generation of the exponentially distributed waiting time until the next event and (ii) random selection of the reaction channel to fire up once the waiting time has elapsed (Gillespie, 1976). We used the SSA to produce the numerical results corresponding to the process determined by the reaction rates given in **Tables S1, S2, S3** and **S4**, as shown in **Figs. 1B-D**, **2A** and **S3**.

A. 2. Semiclassical approximation: optimal reprogramming paths. An alternative way to analyse the dynamics of continuous-time Markov processes on a discrete space of states is to derive an equation for the generating function, $G(p_{1,}\ldots,p_n,t)$ of the corresponding probabilistic density:

$$G(p_{1,}\ldots,p_n,t)=\sum_x p_1^{x_1}p_2^{x_2}\cdots p_n^{x_n}P(x_1,\ldots,x_n,t) \qquad \textbf{[18]}$$

where $P(x_1,\ldots,x_n,t)=P(X,t)$ is the solution of the master equation **(1)**. $P(x_1,\ldots,x_n,t)$ satisfies a partial differential equation that can be derived from the master equation **[1]**. This partial differential equation (PDE) is the basic element of the so-called momentum representation of the master equation **(1)**. The corresponding PDE can be solved explicitly only in a few simple cases. However, although closed analytical solutions are rarely available, the PDE for the generating function admits a Wentzel-Kramers-Brillouin (WKB) perturbative solution (Assaf et al., 2010; Dykman et al., 1995; Kubo et al., 1973).

The (linear) PDE that governs the evolution of the generating function, which is derived from the master equation **(1)** by multiplying both sides by $p_1^{x_1} p_2^{x_2} \cdots p_n^{x_n}$ and summing over all the values of $X = (x_1, \ldots, x_n)$, can be written as follows:

$$\frac{\partial G}{\partial t} = H\left(p_1, \ldots, p_n, \partial_{p_1}, \ldots, \partial_{p_1}\right) G(p_1, \ldots, p_n, t) \qquad \textbf{[19]}$$

where the operator H is determined by the reaction rates of the master equation **[1]**. Furthermore, the solution to this equation must satisfy the normalisation condition $G(p_1 = 1, \ldots, p_n = 1, t) = 1$ for all t. This PDE can be solved analytically only in a few simple cases. However, although closed analytical solutions are rarely available, the PDE for the generating function admits a WKB perturbative solution (Assaf et al., 2010; Dykman et al., 1995; Kubo et al., 1973).

From the mathematical point of view, **[19]** is a Schrödinger-like equation, and, therefore, there is a plethora of methods at our disposal to analyse it. In particular, when the fluctuations are assumed to be small, it is common to resort to WKB perturbation expansion of the solution of **[19]**. This approach is based on the WKB-like Ansatz that $G(p_1, \ldots, p_n, t) = e^{-S(p_1, \ldots, p_n, t)}$. By substituting this Ansatz into **[19]**, we obtain the following Hamilton-Jacobi equation for the action $S(p_1, \ldots, p_n, t)$:

$$\frac{\partial S}{\partial t} = -H\left(p_1, \ldots, p_n, \frac{\partial S}{\partial p_1}, \ldots, \frac{\partial S}{\partial p_n}\right) \qquad \textbf{[20]}$$

Instead of directly seeking the explicit solution of **[20]**, we exploit the Hamilton approach by using the Feynman path-integral representation, which yields a solution to **[19]** of the following type (Feynman and Hibbs, 1965; Dickman and Vidigal, 2003; Täuber et al., 2005):

$$G(p_1, \ldots, p_n, t) = \int_0^t e^{-S(p_1, \ldots, p_n, q_1, \ldots, q_n, s)} Dq(s) Dp(s) \qquad \textbf{[21]}$$

with $S(p_1, \ldots, p_n, q_1, \ldots, q_n)$ given by:

$$S(p_1, \ldots, p_n, t) = \int_0^t \left(- H(p_1, \ldots, p_n, q_1, \ldots, q_n) + \sum_{i=1}^{n} \dot{p}_i(s) q_i(s) \right) + S(p_1, \ldots, p_n, t = 0) \qquad \textbf{[22]}$$

where the position operators in the momentum representation are defined as $q_i \equiv \partial p_1$, with the commutation relation $[p_i, q_j] = \delta_{i,j}$.

The so-called semi-classical approximation consists of approximating the path integral in **[21]** by Sakurai (1994):

$$G(p_1,\ldots,p_n,t) = e^{-S_O\lfloor p_1,\ldots,p_n,t\rfloor} \qquad \textbf{[23]}$$

where $So(p_1,\ldots,p_n,t)$ is the functional action calculated by integrating **[22]** over the solution of the corresponding Hamilton equations, i.e., the orbits that maximise the action S :

$$\frac{dp_i}{dt} = \frac{-\partial H}{\partial q_i} \qquad \textbf{[24]}$$

$$\frac{dq_i}{dt} = \frac{\partial H}{\partial p_i} \qquad \textbf{[25]}$$

where $[q_i, p_j]$ are the generalised coordinates corresponding to chemical species $i = 1,\ldots,n$. These equations are formally solved with boundary conditions $q_i(0) = n_i(0)$ such that $p_i(t) = p$ (Elgart and Kamenev, 2004).

This approach has been recently applied to the analysis of complex protein-interaction systems involving separation of time scales. In particular, the semi-classical approximation has been used to formulate a stochastic version of the quasi-steady approximation (Alarcón, 2014), a framework that we use to simplify the analysis of our system.

A.2.1. Quasi-steady state approximation. The system of Hamilton equations **[24]** and **[25]** with Hamilton given by equations **[A2]** to **[A9]** is far too complex to analyse. To gain insight into the behaviour of the system, we simplify it by performing a quasi-steady state approximation (QSSA). This technique has been extensively used in biochemical modelling (Keener and Sneyd, 1998) and relies on the existence of different time scales whereby one can distinguish between slow and fast variables. Once one has sorted the system variables according to this criterion, one proceeds to make an adiabatic approximation where the fast variables are assumed to be in equilibrium with the slow ones. This procedure reduces the dimension of the system (i.e., number of variables) as well as the number of independent parameters to be determined.

We have recently developed a stochastic QSSA for the semi-classical treatment of complex networks of protein/gene interactions based on the Briggs-Haldane analysis of the Michaelis-Menten system for enzyme catalysis (Alarcón, 2014). According to this analysis, a systematic separation of the system variables into slow and fast can be achieved provided that the number of enzyme molecules is much smaller than the number of substrate molecules. To apply the method put forward in Alarcón (2014) to our current stochastic model, we make the following assumption regarding the characteristic scales for the different values of our stochastic formulation: we assume that the number of all the proteins in our model, i.e., O, S, L_1 and L_2 and their counterparts in the semi-classical approximation q_1, q_3, q_5 and q_7, have

the same characteristic scales, which we denote by y_0. Therefore, once transient regimens have been overcome,

$$x_i = \frac{q_i}{y_0} = O(1), i = 1,3,5,7 \qquad \textbf{[26]}$$

We further assume that the quantities T_O, T_S, T_1 and T_2 (see equations **[13]** to **[16]**) are all of the same order of magnitude and all have the same characteristic scale, T_O. T_O is the natural scale for the variables corresponding to the free and bound binding sites in the gene promoter regions as well as for the epigenetic regulation variables (M_i, U_i and A_i or the counterparts $q_i, i = 22, ..., 27$), i.e.,:

$$x_i = \frac{q_i}{T_0} = O(1), i \neq 1,3,5,7 \qquad \textbf{[27]}$$

The separation of time scales necessary to apply the QSSA emerges if we assume the following:

$$\varepsilon = T_0 << 1 \qquad \textbf{[28]}$$

To proceed further, we consider the Hamilton equations **[24]** and **[25]** and re-scale the time variable, $\tau = k_{11} T_0 y_0^2 t$, and the Hamiltonian $H_k(p,q) = k_{11} T_0 y_0^2 H_\kappa(p,x)$, where x_i are the re-scaled variables defined in **[26]** and **[27]**. When re-scaling the Hamiltonian, the parameters k_i featured in **[A4]** and **[A9]** must also be re-scaled and are thus substituted by the corresponding parameters κ_i given in **Table S6**. For simplicity, we split the re-scaled Hamiltonian into two contributions, $H_\kappa(p,x) = H_{GR}(p,x) + H_{ER}(p,x)$, which we analyse separately. $H_{GR}(p,x) = H_{SD}(p,x) + H_{P_O}(p,x) H_{P_S}(p,x) + \sum_i H_{P_i}(p,x)$ is the Hamiltonian associated with gene regulation, and $H_{ER}(p,x) = \sum_i H_{E_i}(p,x)$ is the Hamiltonian corresponding to the epigenetic regulation of the *LSGs*.

Table S6

Re-scaled parameter	
$\rho_1 = \frac{R_1}{k_{11} T_0 y_0^2}$	
$\kappa_i = \frac{k_i}{k_{11} T_0 y_0}$	If i=2,4,6,8

$\kappa_i = \frac{k_i}{k_{11}}$	If i=13,15,17,19,21,23,25,27,29,31,33,35
$\kappa_i = \frac{k_i T_0}{k_{11} y_0}$	If i=35+8(j-1),36+8(j-1),37+8(j-1),38+8(j-1), j=1,2
$\kappa_i = \frac{k_i}{k_{11} y_0}$	If i=39+8(j-1),40+8(j-1),41+8(j-1),42+8(j-1), j=1,2
$\kappa_i = \frac{k_i}{k_{11} y_0^2}$	otherwise

Re-scaled parameters that result upon re-scaling of the Hamiltonian (A2): $H_k(p,q) = k_{11} T_0 y_0^2 H_\kappa(p,x)$

The QSSA for the gene regulation Hamiltonian, $H_{GR}(p,x)$, derived in detail in **Appendix B**, is given by the following system of ordinary differential equations:

$$\frac{dx_1}{d\tau} = \rho_1 + p_2 \frac{\kappa_1}{\kappa_{12}} \frac{\vartheta_O x_1 x_3}{1 + \frac{1}{\kappa_{12}} x_1 x_3 + \frac{\kappa_{13}}{\kappa_{14}} x_5^2 + \frac{\kappa_{15}}{\kappa_{16}} x_7^2} - \kappa_2 x_1 \qquad \textbf{[29]}$$

$$\frac{dx_3}{d\tau} = \rho_1 + p_4 \kappa_3 \frac{\kappa_{17}}{\kappa_{18}} \frac{\vartheta_S x_1 x_3}{1 + \frac{\kappa_{17}}{\kappa_{18}} x_1 x_3 + \frac{\kappa_{19}}{\kappa_{20}} x_5^2 + \frac{\kappa_{21}}{\kappa_{22}} x_7^2} - \kappa_4 x_3 \qquad \textbf{[30]}$$

$$\frac{dx_5}{d\tau} = p_6 \kappa_5 \frac{\kappa_{25}}{\kappa_{26}} \frac{\vartheta_1(x_{24}) x_5^2}{1 + \frac{\kappa_{23}}{\kappa_{24}} x_1 x_3 + \frac{\kappa_{25}}{\kappa_{26}} x_5^2 + \frac{\kappa_{27}}{\kappa_{28}} x_7^2} - \kappa_6 x_5 \qquad \textbf{[31]}$$

$$\frac{dx_7}{d\tau} = p_8 \kappa_7 \frac{\kappa_{31}}{\kappa_{32}} \frac{\kappa_2(x_{27}) x_7^2}{1 + \frac{\kappa_{29}}{\kappa_{30}} x_1 x_3 + \frac{\kappa_{33}}{\kappa_{34}} x_5^2 + \frac{\kappa_{31}}{\kappa_{32}} x_7^2} - \kappa_8 x_7 \qquad \textbf{[32]}$$

for the re-scaled number of Oct4, Sox2, LSG1 and LSG2 proteins, respectively, where we have defined $\vartheta_O = T_O / T_0$, $\vartheta_S = T_S / T_0$, $\vartheta_1 = T_1 / T_0$, and $\vartheta_2 = T_2 / T_0$. It should be noted that x_{24} and x_{27} are the re-scaled canonical coordinates corresponding to A_1 and A_2, i.e., the acetylation levels of LSG1 and LSG2, respectively. The corresponding QSSA for the momenta yields the following results:

$$p_1 = p_3 = p_5 = p_7 = 1 \qquad \textbf{[33]}$$

$$p_2 = p_{10} = p_{11} = p_{12} = c_O \qquad \textbf{[34]}$$

$$p_4 = p_{13} = p_{14} = p_{15} = c_S \qquad \textbf{[35]}$$

$$p_6 = p_{16} = p_{17} = p_{18} = c_1 \quad \textbf{[36]}$$

$$p_8 = p_{19} = p_{20} = p_{21} = c_2 \quad \textbf{[37]}$$

where c_O, c_S, c_1, c_2 are given in **Appendix C**, where we show that they are determined by the distribution of the number of binding sites in the promoter region of the respective genes in a population of cells.

To close the QSSA system equations **[29]** to **[32]**, it is necessary to determine the dynamic of x_{24} and x_{27}, for which we turn now to the analysis of the epigenetic Hamiltonian, $H_{ER}(p,x) = H_{E_1}(p,x) + H_{E_2}(p,x)$ (see **Appendix A**). A direct numerical solution of the corresponding Hamilton equations **[24]** and **[25]** shows that for x_{22}, x_{26} and x_{27} to remain positive, the corresponding momenta must satisfy the following:

$$p_{22} = p_{23} = p_{24} = const. = c_{E_1} \quad \textbf{[38]}$$

$$p_{25} = p_{26} = p_{27} = const. = c_{E_2} \quad \textbf{[39]}$$

where the constants c_{E_1} and c_{E_2} are resolved in **Appendix C**, where we show that they are determined by the distribution of the number of modification sites in the nucleosomes of the respective genes in a population of cells. Considering this fact, we can write the corresponding evolution equations for x_{22}, x_{23} and x_{24} and x_{25}, x_{26} and x_{27}:

$$\frac{dx_{22}}{d\tau} = -\kappa_{35} h_2 c_{E_1} x_{22} x_{24} - \kappa_{39} x_{22} + \kappa_{36} h_1 c_{E_1} x_{22} x_{23} + \kappa_{41} h_1 x_{23} \quad \textbf{[40]}$$

$$\frac{dx_{24}}{d\tau} = -\kappa_{37} h_{24} c_{E_1} x_{22} x_{24} - \kappa_{40} x_{24} + \kappa_{38} h_3 c_{E_1} x_{24} x_{23} + \kappa_{42} h_3 x_{23} \quad \textbf{[41]}$$

$$x_{23} = 1 - x_{22} - x_{24} \quad \textbf{[42]}$$

and

$$\frac{dx_{25}}{d\tau} = -\kappa_{43} h_4 c_{E_2} x_{25} x_{26} - \kappa_{47} x_{25} + \kappa_{44} h_1 c_{E_2} x_{25} x_{27} + \kappa_{49} h_1 x_{26} \quad \textbf{[43]}$$

$$\frac{dx_{27}}{d\tau} = -\kappa_{45} h_4 c_{E_2} x_{25} x_{27} - \kappa_{48} x_{27} + \kappa_{46} h_3 c_{E_2} x_{27} x_{26} + \kappa_{50} h_3 x_{26} \quad \textbf{[44]}$$

$$x_{26} = 1 - x_{25} - x_{27} \quad \textbf{[45]}$$

respectively.

A. 3. Parameter values

The last element that remains to be addressed regarding our model formulation concerns the values of the biophysical parameters (e.g., binding and unbinding rates, protein synthesis and degradation rates) that determine the behaviour of our system. To fix the value of the parameters in our model, we require the following three properties be satisfied:

(1) The epigenetic regulation models, equations **[40]** and **[41]** and **[43]** to **[45]**, should be in their bistable regimes, where two stable steady states corresponding to methylated and acetylated states exist.

(2) A baseline scenario must exist where the acetylated states of both *LSGs* are the more stable ones, which, in turn, should give rise to cells that exist in a differentiated state.

(3) The gene regulation model, equations **[29]** to **[32]**, must be such that, in the baseline scenario, three stable steady-states exist: a pluripotent state, x_p^*, such that the stemness-related genes (*OCT4* and *SOX2*) have positive levels of expression and the *LSGs* are not being expressed, and two differentiation states, x_1^* and x_2^*, where *LSG1* and *LSG2*, respectively, have positive levels of expression, whereas all the other genes have vanishing levels of expression.

Our so-called baseline scenario is characterised by (i) normal levels of the oncometabolite 2HG (i.e., normal activity of the histone de-methylating enzymes) and (ii) no induction of the stemness-related genes (i.e., $\rho_1 = \rho_2 = 0$). These requirements are not sufficient to uniquely determine the values of all the parameters in our model, but they help us establish the region of parameter values where our stochastic model makes biological sense.

To further simplify the analysis and without loss of generality in our results, we assume the following: (i) all the dimer-promoter binding constants are the same; (ii) all the dimer-promoter unbinding constants are the same; (iii) all the gene products are synthesised at the same time; and (iv) all the proteins are degraded at the same rate. We make a similar simplifying assumption regarding the epigenetic regulatory system, namely, that all the rates corresponding to recruited modification have the same value. Similarly, all the rates of unrecruited modification are assumed to have the same value.

The conditions that the parameter values of our stochastic model must satisfy for the three properties listed above are derived in **Appendix D** and **Appendix E**. Parameter values satisfying such conditions and compatible with the baseline scenario are given in **Table S7**.

B. Experiments on living cells

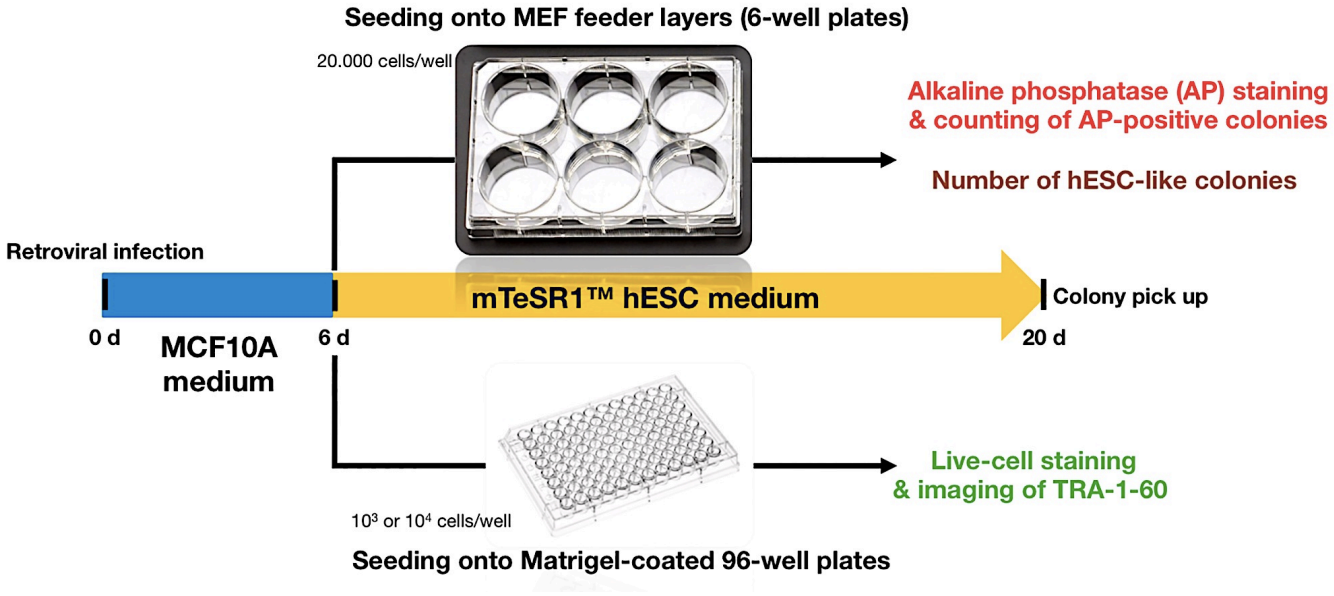

Figure S1. A timeline for the overall iPS cell derivation protocol employed in the proof-of-concept validation experiments on living cells is outlined.

Supplemental appendices

APPENDIX A. The Hamiltonian function

As the master equation **[1]** is linear, we can arrange it by splitting its right-hand side operator as follows:

$$\frac{\partial P(X,t)}{\partial t} = \sum_{i=1}^{8} W_i(X - r_i)P(X - r_i,t) - W_i(X)P(X,t)$$
$$+ \sum_{i=11}^{16} W_i(X - r_i)P(X - r_i,t) - W_i(X)P(X,t)$$
$$+ \sum_{i=17}^{22} W_i(X - r_i)P(X - r_i,t) - W_i(X)P(X,t)$$
$$+ \sum_{i=23}^{28} W_i(X - r_i)P(X - r_i,t) - W_i(X)P(X,t)$$
$$+ \sum_{i=29}^{34} W_i(X - r_i)P(X - r_i,t) - W_i(X)P(X,t)$$
$$+ \sum_{i=35}^{42} W_i(X - r_i)P(X - r_i,t) - W_i(X)P(X,t)$$
$$+ \sum_{i=43}^{50} W_i(X - r_i)P(X - r_i,t) - W_i(X)P(X,t) \qquad \textbf{[A1]}$$

where the first summation corresponds to the processes described in **Table S4**, i.e., protein synthesis and degradation. The second to fifth summations correspond to the competitive binding to the gene promoters as given in **Tables S1**, **S2** and **S3**. The last two summations in **[A1]** correspond to the dynamics of epigenetic regulation of each of the LSGs and are determined by the rates given in **Table S5**.

To obtain the corresponding Hamiltonian, we begin by multiplying both sides of **[A1]** by $p_{21},\ldots,p_{27}$ and sum over all the possible values of the state vector $X = (O, S, \ldots, U_2, A_2)$. This procedure yields a partial differential equation for the probability generating function, $G(p_{21},\ldots,p_{27})$, of the type of equation **[19]**, where the time evolution of the generating function is driven by the operator $G(p_{21},\ldots,p_{27},\partial_{p1},\ldots,\partial_{p27})$. The representation of this operator where ∂_{pi} are represented by $q_i = \partial_{pi}$ yields the Hamiltonian corresponding to **[A1]**. Following the arrangement of **[A1]**, the Hamiltonian $H_\kappa(p,q)$, can be written as follows:

$$H_\kappa(p,x) = H_{SD}(p,x) + H_{P_O}(p,x)H_{P_S}(p,x) + \sum_i H_{P_i}(p,x) + H_{E_i}(p,x) \qquad \textbf{[A2]}$$

where $H_{P_O}(p,q)$, $H_{P_S}(p,q)$, $H_{Pi}(p,q)$, $H_{SD}(p,q)$ and $H_{E_i}(p,q)$ are the Hamiltonians corresponding to the processes described in **Tables S1**, **S2**, **S3**, **S4** and **S5**, respectively. These Hamiltonians can be easily computed from **[A1]** and are given by:

$$\begin{aligned}H_{SD}(p,q) &= k_1 p_2 (p_1 - 1) q_2 + R(p_1 - 1) + \\ & k_2 (1 - p_1) q_1 + k_3 p_4 (p_3 - 1) q_4 + R(p_3 - 1) + k_4 (1 - p_3) q_3 \\ & + k_5 p_6 (p_5 - 1) q_6 + k_6 (1 - p_5) q_6 + k_7 p_8 (p_7 - 1) q_8 + k_8 (1 - p_7) q_7 \end{aligned} \quad \textbf{[A3]}$$

where the pairs (p_i, q_i) with $i = 1, \ldots, 8$ are the generalised coordinates corresponding to O, $B_{O,O-S}$, S, $B_{S,O-S}$, L_1, $B_{1,1-1}$, L_2 and $B_{2,2-2}$, respectively,

$$\begin{aligned}H_{P_O}(p,q) &= k_{11}(p_2 - p_9 p_{10}) q_9 q_{10} + \\ & k_{12}(p_9 p_{10} - p_2) q_2 + k_{13}(p_{11} - p_5^2 p_{10}) q_5^2 q_{10} + k_{14}(p_5^2 p_{10} - p_{11}) q_{11} \\ & + k_{15}(p_{12} - p_7^2 p_{10}) q_7^2 q_{10} + k_{16}(p_7^2 p_{10} - p_{12}) q_{12} \end{aligned} \quad \textbf{[A4]}$$

where (p_i, q_i), $i = 10, 11, 12$ are the generalised coordinates corresponding to F_O, $B_{O,1-1}$ and $B_{O,2-2}$, respectively,

$$\begin{aligned}H_{P_S}(p,q) &= k_{14}(p_4 - p_9 p_{13}) q_9 q_{13} + \\ & k_{18}(p_9 p_{10} - p_4) q_4 + k_{19}(p_{14} - p_5^2 p_{13}) q_5^2 q_{13} + k_{20}(p_5^2 p_{13} - p_{14}) q_{14} \\ & + k_{21}(p_{15} - p_7^2 p_{13}) q_7^2 q_{13} + k_{22}(p_7^2 p_{10} - p_{15}) q_{15} \end{aligned} \quad \textbf{[A5]}$$

where (p_i, q_i), $i = 13, 14, 15$ are the generalised coordinates corresponding to F_S, $B_{S,1-1}$ and $B_{S,2-2}$, respectively,

$$\begin{aligned}H_{P_1}(p,q) &= k_{23}(p_{18} - p_9 p_{16}) q_9 q_{16} + \\ & k_{24}(p_9 p_{16} - p_{18}) q_{18} + k_{25}(p_6 - p_5^2 p_{16}) q_5^2 q_{16} + k_{26}(p_5^2 p_{13} - p_6) q_6 \\ & + k_{27}(p_{17} - p_7^2 p_{16}) q_7^2 q_{16} + k_{28}(p_7^2 p_{16} - p_{17}) q_{17} \end{aligned} \quad \textbf{[A6]}$$

$$\begin{aligned}H_{P_2}(p,q) &= k_{29}(p_{21} - p_9 p_{19}) q_9 q_{19} + \\ & k_{30}(p_9 p_{19} - p_{21}) q_{21} + k_{31}(p_8 - p_7^2 p_{19}) q_7^2 q_{19} + k_{32}(p_7^2 p_{19} - p_8) q_8 \\ & + k_{33}(p_{20} - p_5^2 p_{19}) q_5^2 q_{19} + k_{34}(p_5^2 p_{19} - p_{20}) q_{20} \end{aligned} \quad \textbf{[A7]}$$

where the pairs $(p_i\ ,\ q_i)$ with $i = 16, \ldots, 21$ are the generalised coordinates corresponding to F_1, $B_{1,2-2}$, $B_{1,O-S}$, F_2, $B_{2,1-1}$ and $B_{2,O-S}$ respectively. Finally, the Hamiltonian functions corresponding to the epigenetic regulation of the *LSGs* (see **Table S5**) are given by:

$$H_{E_1}(p,q) = (p_{23} - p_{22})(k_{35}h_2 p_{24}q_{22}q_{24} + k_{39}q_{22}) + (p_{22} - p_{23})(k_{36}h_1 p_{22}q_{22}q_{23} + k_{41}h_1 q_{23}) + (p_{23} - p_{24})(k_{37}h_4 p_{22}q_{22}q_{24} + k_{40}q_{24}) + (p_{23} - p_{24})(k_{38}h_3 p_{24}q_{22}q_{24} + k_{42}h_3 q_{23}) \quad \textbf{[A8]}$$

$$H_{E_2}(p,q) = (p_{26} - p_{25})(k_{35}h_2 p_{27}q_{25}q_{27} + k_{39}q_{25}) + (p_{25} - p_{26})(k_{36}h_1 p_{25}q_{25}q_{26} + k_{41}h_1 q_{26}) + (p_{26} - p_{27})(k_{37}h_4 p_{25}q_{25}q_{27} + k_{40}q_{27}) + (p_{27} - p_{26})(k_{38}h_3 p_{27}q_{25}q_{27} + k_{42}h_3 q_{26}) \quad \textbf{[A9]}$$

The pairs $(p_i\ ,\ q_i)$ with $i = 22, \ldots, 27$ appearing in **[A8]** and **[A9]** are the generalised coordinates corresponding to M_1, U_1, A_1, M_2, U_2 and A_2, respectively.

APPENDIX B. QSSA of the Hamilton equations for the gene regulation Hamiltonian

We begin QSSA analysis by studying the gene regulation Hamiltonian, $H_{GR}(p,x)$. By introducing re-scaled variables and the re-scaled gene regulation Hamiltonian in **[24]** and **[25]**, we obtain:

$$s_i \frac{dp_i}{dt} = -y_0 \frac{\partial H_{GR}}{\partial x_i} \quad \textbf{[B1]}$$

$$s_i \frac{dx_i}{d\tau} = y_0 \frac{\partial H_{GR}}{\partial p_i} \quad \textbf{[B2]}$$

where $i = 1, \ldots, 21$ (i.e., all the variables except the ones characterising the epigenetic states of the *LSGs*) and

$s_i = y_0$ if $i = 1,3,5,7$ (T_0 otherwise), **[B3]**

which separates the variables of our system into slow variables:

$$\frac{dp_i}{d\tau} = \frac{-\partial H_{GR}}{\partial x_i} \quad \textbf{[B4]}$$

$$\frac{dx_i}{d\tau} = \frac{\partial H_{GR}}{\partial p_i} \quad \textbf{[B5]}$$

$i = 1,3,5,7$, and fast variables:

$$\varepsilon \frac{dp_i}{d\tau} = \frac{-\partial H_{GR}}{\partial x_i} \qquad \textbf{[B6]}$$

$$\varepsilon \frac{dx_i}{d\tau} = \frac{\partial H_{GR}}{\partial p_i} \qquad \textbf{[B7]}$$

otherwise. Finally, the QSSA system is given by:

$$\frac{dp_i}{d\tau} = \frac{-\partial H_{GR}}{\partial x_i} \qquad \textbf{[B8]}$$

$$\frac{dx_i}{d\tau} = \frac{\partial H_{GR}}{\partial p_i} \qquad \textbf{[B9]}$$

$$0 = \frac{-\partial H_{GR}}{\partial x_i} \qquad \textbf{[B10]}$$

$$0 = \frac{\partial H_{GR}}{\partial p_i} \qquad \textbf{[B11]}$$

for $i \neq 1,3,5,7$.

In addition, we also have several constraints that help us solve the QSSA system **[B8]** and **[B9]**:

(i) Our system is conservative, and therefore $H_{GR}\left(p(t),x(t)\right)$ must be constant along the solutions of **[B8]** and **[B9]**, i.e., $H_{GR}\left(p(t),x(t)\right) = E_{GR}$. E_{GR} is an arbitrary quantity, so for simplicity, we choose $E_{GR} = 0$.

(ii) We also need to consider the constraints regarding the number of binding sites in each promoter region. In re-scaled variables, **[13]** to **[16]** read:

$$x_2 + x_{10} + x_{11} + x_{12} = \vartheta_O \qquad \textbf{[B12]}$$

$$x_4 + x_{13} + x_{14} + x_{15} = \vartheta_S \qquad \textbf{[B13]}$$

$$x_6 + x_{16} + x_{17} + x_{18} = \vartheta_1 \qquad \textbf{[B14]}$$

$$x_8 + x_{19} + x_{20} + x_{21} = \vartheta_2 \qquad \textbf{[B15]}$$

where $\vartheta_O = T_O / T_{0,}\ \vartheta_S = T_S / T_{0,}\ \vartheta_1 = T_1 / T_{0,}$ and $\vartheta_2 = T_2 / T_0$. It is easy to verify from **[B10]** and **[B11]** with $i =$ 2,4,6,8 that for the conservation laws **[B12]** to **[B15]** to hold, $p_1 + p_3 + p_5 + p_7 = 1$must be satisfied.

It is also easy to verify that **[B8]** to **[B11]** imply that $H_{P_O}(p,x)=H_{P_S}(p,x)=H_{P_1}(p,x)=H_{P_2}(p,x)=0$. Therefore, under QSSA conditions, the gene regulation Hamiltonian reduces to:

$$H_{GR}(p,q)\approx H_{SD}(p,q)=k_1p_2(p_1-1)q_2+R \qquad \textbf{[B16]}$$

$$(p_1-1)+k_2(1-p_1)q_1+k_3p_4(p_3-1)q_4+R(p_3-1)+k_4(1-p_3)q_3 \qquad \textbf{[B17]}$$

$$+k_5p_6(p_5-1)q_6+k_6(1-p_5)q_6+k_7p_8(p_7-1)q_8+k_8(1-p_7)q_7$$

which implies that the condition $E_{GR}=0$ is trivially satisfied when $p_1+p_3+p_5+p_7=1$. Furthermore, **[B11]** for $i=2,11,12$, read:

$$\kappa_1p_2(1-p_1)+\kappa_{12}(p_1-p_1p_3p_{10})=0 \qquad \textbf{[B18]}$$

$$\kappa_{14}(p_{11}-p_5^2p_{10})=0 \qquad \textbf{[B19]}$$

$$\kappa_{16}(p_{12}-p_7^2p_{10})=0 \qquad \textbf{[B20]}$$

which, because $p_1+p_3+p_5+p_7=1$, reduces to $p_2+p_{10}+p_{11}+p_{12}=c_O$ where c_O is a constant to be determined later in our calculation. Similarly, the fact that $p_1+p_3+p_5+p_7=1$ implies that:

$$p_4=p_{13}=p_{14}=p_{15}=c_S \qquad \textbf{[B21]}$$

$$p_6=p_{16}=p_{17}=p_{18}=c_1 \qquad \textbf{[B22]}$$

$$p_8=p_{19}=p_{20}=p_{21}=c_2 \qquad \textbf{[B23]}$$

where c_S, c_1 and c_2 are constants to be determined later.

To proceed further, consider **[B8]**, which reduces to:

$$\frac{dx_1}{d\tau}=\rho_1+\kappa_1p_2x_2-\kappa_2x_1 \qquad \textbf{[B24]}$$

$$\frac{dx_3}{d\tau}=\rho_1+\kappa_3p_4x_4-\kappa_4x_3 \qquad \textbf{[B25]}$$

$$\frac{dx_5}{d\tau}=\kappa_5p_6x_6-\kappa_6x_5 \qquad \textbf{[B26]}$$

$$\frac{dx_7}{d\tau}=\kappa_7p_8x_8-\kappa_8x_7 \qquad \textbf{[B27]}$$

Let us focus on **[B24]**, which determines the time evolution of x_1. Moreover, according to **[B10]** with $i=2,11,12$, we have:

$$x_2 = \frac{1}{\kappa_{12}} x_1 x_3 x_{10} \qquad \textbf{[B28]}$$

$$x_{11} = \frac{\kappa_{13}}{\kappa_{14}} x_5^2 x_{10} \qquad \textbf{[B29]}$$

$$x_{12} = \frac{\kappa_{15}}{\kappa_{16}} x_7^2 x_{10} \qquad \textbf{[B30]}$$

[B12] and **[B28]** enable us to write x_{10} as a function of x_1, x_3, x_5 and x_7:

$$x_{10} = \frac{\vartheta_O}{1 + \frac{1}{\kappa_{12}} x_1 x_3 + \frac{\kappa_{13}}{\kappa_{14}} x_1 x_3 + \frac{\kappa_{15}}{\kappa_{16}} x_7^2} \qquad \textbf{[B31]}$$

which, in turn, enables us to express x_2 as a function of x_1, x_3, x_5 and x_7:

$$x_2 = \frac{1}{\kappa_{12}} \frac{\vartheta_O x_1 x_3}{1 + \frac{1}{\kappa_{12}} x_1 x_3 + \frac{\kappa_{13}}{\kappa_{14}} x_5^2 + \frac{\kappa_{15}}{\kappa_{16}} x_7^2} \qquad \textbf{[B32]}$$

Finally, **[B24]** and **[B32]** lead to **[29]**. The derivation of equations **[30]** to **[32]** is completely analogous.

APPENDIX C. Determination of the values and physical interpretation of p_2, p_4, p_6 and p_8

This appendix is devoted to determining the values of the constants p_2, p_4, p_6 and p_8, which we need to close the QSSA of our system given by equations **[29]** to **[32]**. The procedure to calculate the value of these quantities also enables us to describe a physical interpretation of their meaning.

Using the fact that $E_{GR} = 0$ and interpreting by parts, we can re-write the action functional S **[22]** as follows:

$$S_{GR}(p_1, \ldots, p_{21}, \tau) = y_0 \sum_{i=1}^{21} \int_0^{\tau} x_i(s) \left(\frac{s_i}{y_0} \frac{dp_i}{ds} \right) ds + S(p_1, \ldots, p_{21}, \tau = 0) \qquad \textbf{[C1]}$$

where s_i is defined in **[B3]**. As the QSSA implies that $p_i = constant$ for all i, the QSSA approximation of **[C1]**, $S_{GRQ}(p,t)$, reduces to:

$$S_{GRQ}(p_{1,}\ldots,p_{21,}\tau)=S_{GRQ}(p_{1,}\ldots,p_{21,}\tau=0) \qquad \textbf{[C2]}$$

We further assume that the initial value of each of the state variables is an independent random variable, which implies that $S_{GRQ}(p_{1,}\ldots,p_{21,}\tau)=\sum_{i=1}^{21} S_i(p_{i,})$. As $p_1 = p_3 = p_5 = p_7 = 1$, the corresponding functions $S_1 = S_3 = S_5 = S_7 = 0$. The resulting $S_{GRQ}(p,\tau)$ can therefore be written as:

$$S_{GRQ}(p_{21,}\ldots,p_{21,}\tau)=S_O(c_O)+S_S(c_S)+S_{L_1}(c_1)+S_{L_2}(c_2) \qquad \textbf{[C3]}$$

where $S_O(c_O)$ is the negative of the logarithm of the generating function of the probability density of the total number of binding sites within the promoter of *OCT4*. $S_S(c_S), S_{L_1}(c_1)$ and $S_{L_2}(c_2)$ are the corresponding quantities for the total number of binding sites in the promoters of *SOX2*, *LSG1* and *LSG2*, respectively. To obtain this result, we used **[B21]** and the well-known fact regarding the properties of the generating function of a random variable $G_N(p)$, which is the sum of n independent random variables given by:

$$G_N(p)=\prod_{i=1}^{n} G_i(p) \qquad \textbf{[C4]}$$

where $G_i(p)$ is the generating function of the probability density of each independent random variable (Grimmett and Stirzaker, 1992).

As **[C3]** implies that the total number of binding sites in each of the four promoters is an independent random variable, we can proceed to calculate, say, c_O by setting $c_S = c_1 = c_2 = 1$, i.e., $S_S(c_S=1)=S_{L_1}(c_1=1)+S_{L_2}(c_2=1)=0$, which is equivalent to taking the marginal probability of the number of binding sites in the promoter of *OCT4*, b_O . The calculation of the other three quantities, $c_S, c_1,$ and c_2 , is completely analogous.

As an immediate consequence of the definition of the probability generation function, one can use Cauchy's formula to obtain the probability of the number of binding sites in the promoter of *OCT4*, b_O , i.e., (*2*)

$$P(b_O,\tau)=\frac{1}{2\pi i}\oint\left(\frac{G_O(p,\tau)}{p^{b_O+1}}\right)dp=\frac{1}{2\pi i}\oint\left(\frac{e^{-S_O(p,\tau)}}{p^{b_O+1}}\right)dp=\frac{1}{2\pi i}\oint\left(\frac{e^{-S_O(p,\tau)-b_O\log(p)}}{p}\right)dp \qquad \textbf{[C5]}$$

Let us now define the function $f(p)$through the relation $E_{Of}(p) = E_O\left(s_O(p) + \frac{b_O}{E_O}\log p\right)$, where E_O is the average of the total number of binding sites in the promoter of *OCT4*.

$$P(b_O, \tau) = \frac{1}{2\pi i}\oint\left(\frac{e^{-E_O f(p)}}{p}\right)dp \qquad \textbf{[C6]}$$

If $E_O >> 1$, then we can apply the method of Laplace (or the method of the stationary phase) to approximately solve the integral (Ablowitz and Fokas, 2003; Murray, 1984). According to this method, if $E_O >> 1$, the only contribution to the integral corresponds to the value of $p = c_O$ for which $f(p)$exhibits a maximum. The value of c_O is therefore found by maximising $f(p)$, i.e.:

$$c_O\left|\frac{ds_O}{dp}\right|_{p=c_O} = \frac{-b_O}{E_O} \qquad \textbf{[C7]}$$

Similarly,

$$c_S\left|\frac{ds_S}{dp}\right|_{p=c_S} = \frac{-b_S}{E_S} \qquad \textbf{[C8]}$$

$$c_1\left|\frac{ds_1}{dp}\right|_{p=c_1} = \frac{-b_1}{E_1} \qquad \textbf{[C9]}$$

$$c_2\left|\frac{ds_2}{dp}\right|_{p=c_2} = \frac{-b_2}{E_2} \qquad \textbf{[C10]}$$

If we consider that the number of binding sites in each of the four promoters is distributed according to a Poisson distribution, we have the following:

$$S_O(p) = -E_O(p-1), s_O(p) = -(p-1) \qquad \textbf{[C11]}$$

$$S_S(p) = -E_S(p-1), s_S(p) = -(p-1) \qquad \textbf{[C12]}$$

$$S_1(p) = -E_1(p-1), s_1(p) = -(p-1) \qquad \textbf{[C13]}$$

$$S_2(p) = -E_2(p-1), s_2(p) = -(p-1) \qquad \textbf{[C14]}$$

which, according to equations **[C7]** to **[C10]**, yields $c_O = \frac{b_O}{E_O}, c_S = \frac{b_S}{E_S}, c_1 = \frac{b_1}{E_1}, c_2 = \frac{b_2}{E_2}$.

Physical interpretation. The derivation of the previous section implies that the values of c_O, c_S, c_1 and c_2 are determined by the probability distribution of binding sites in the promoter of the corresponding gene.

The interpretation of this result is that these quantities are non-uniformly distributed over a population of cells. Thus, we look at a population of cells, the proportion of cells with a given number of binding sites in the promoter of, say, *OCT4* is given by **[C6]**. In other words, each cell randomly picked from such population will have a different value of binding sites in the *OCT4* promoter distributed according to **[C6]**. In the particular case that the number of binding sites is distributed according to a Poisson distribution, we find that, for example, c_O depends on the ratio between the actual binding sites in a cell within the population, b_O , and its average over the population, so that individual cells are characterised by a parameter that is determined by whether its number of binding sites in the *OCT4* promoter is above, exactly equal to, or below average.

Appendix C1. Determination of C_{E_1} and C_{E_2}

To determine the values of the constants C_{E_1} and C_{E_2} , we follow the same general procedure as in the previous case. In the main text, we have established that for x_{22}, x_{23} and x_{24} and x_{25} , x_{26} and x_{27} to be positive, the corresponding momenta must satisfy:

$$p_{22} = p_{23} = p_{24} = const. = c_{E_1} \qquad \textbf{[C15]}$$

$$p_{25} = p_{26} = p_{27} = const. = c_{E_2} \qquad \textbf{[C16]}$$

These equations have the consequence that $E_{ER} = H_{ER}(p,x) = 0$ (see equations **[A6]** and **[A7]**), which implies, in turn, that the corresponding action functional, $S_{ER}(p,t)$, can be expressed as:

$$S_{ER}\left(p_{22,}\ldots,p_{27},\boldsymbol{\tau}\right) = y_0 \sum_{i=22}^{27} \int_0^{\tau} x_i(s)\left(\frac{s_i}{y_0}\frac{dp_i}{d\boldsymbol{\tau}}\right)ds + S_{E_1}\left(p_{22,}\ldots,p_{24},\boldsymbol{\tau}=0\right) + S_{E_1}\left(p_{25,}\ldots,p_{27},\boldsymbol{\tau}=0\right) \qquad \textbf{[C17]}$$

where s_i is given by **[B3]**. Furthermore because all the momenta in **[C17]** are constant, the epigenetic regulation action, $S_{ER}\left(p_{22,}\ldots,p_{27},\boldsymbol{\tau}\right)$, reduces to:

$$S_{ER}\left(p_{22,}\ldots,p_{27},\boldsymbol{\tau}\right) = S_{E_1}\left(p_{22,}\ldots,p_{24},\boldsymbol{\tau}=0\right) + S_{E_2}\left(p_{25,}\ldots,p_{27},\boldsymbol{\tau}=0\right) \qquad \textbf{[C18]}$$

Following the same procedure as in the previous section, we finally obtain that C_{E_1} *and* C_{E_2} are given by:

$$c_{E_1}\left|\frac{ds_{E_1}}{dp}\right|_{p=c_{E_1}} = \frac{-b_{E_1}}{E_{E_1}} \qquad \textbf{[C19]}$$

$$c_{E_2}\left|\frac{ds_{E_2}}{dp}\right|_{p=c_{E_2}} = \frac{-b_{E_2}}{E_{E_2}} \qquad \textbf{[C20]}$$

where $S_{E_1}(p) = E_{E_1} s_{E_1}(p)$ is the negative of the logarithm of the generating function of the probability density function of the number of modification sites of the *LSG1* gene (reciprocally, for *LSG2*).

The physical interpretation is also analogous to the one in the previous section, namely, each cell randomly picked from a cell population will have a different number of modification sites in *LSG1* and *LSG2,* distributed according to the corresponding probability distribution function.

Again, if the number of modification sites in *LSG1* and *LSG2* is distributed according to a Poisson distribution, then $c_{E_1} = \frac{b_{E_1}}{E_{E_1}}$ and $c_{E_2} = \frac{b_{E_2}}{E_{E_2}}$.

APPENDIX D. Stability analysis of the epigenetic regulation model in the baseline scenario

To simplify our analysis, and without loss of generality, we assume that $\kappa_{35} = \kappa_{36} = \kappa_{37} = \kappa_{38} = d_1$ and $\kappa_{39} = \kappa_{40} = \kappa_{41} = \kappa_{42} = d_2$ Similarly, $\kappa_{43} = \kappa_{44} = \kappa_{45} = \kappa_{46} = d_1$ and $\kappa_{47} = \kappa_{48} = \kappa_{49} = \kappa_{50} = d_2$. The steady states of the system will be expressed as given by $x^* = (1-\alpha-\beta, \alpha, \beta)$, where α and β are the steady-state values of x_{23} (normalised number of unmodified sites) and x_{24} (normalised number of acetylated sites), respectively, which must satisfy:

$$-d_1 h_2 c_{E_1}(1-\alpha-\beta)\beta - d_2(1-\beta-\alpha) + d_1 h_1 c_{E_1}(1-\alpha-\beta)\alpha + d_2 h_1 \alpha = 0 \qquad \textbf{[D1]}$$

$$-d_1 h_4 c_{E_1}(1-\alpha-\beta)\beta - d_2\beta + d_1 h_3 c_{E_1}\beta\alpha + d_2 h_3 \alpha = 0 \qquad \textbf{[D2]}$$

The number of steady states is determined by the intersections between the null-clines:

$$-d_1 h_2 c_{E_1}(1-\alpha-\beta)\beta - d_2(1-\beta-\alpha) + d_1 h_1 c_{E_1}(1-\alpha-\beta)\alpha + d_2 h_1 \alpha = 0 \qquad \textbf{[D3]}$$

$$\alpha = \frac{d_1 h_4 c_{E_1}(1-\beta)\beta + d_\beta}{d_1 c_{E_1}(h_3 + h_4)\beta + d_2 h_3} \qquad \textbf{[D4]}$$

The result is illustrated in **Fig. S2**, in which we show the null-clines for different values of the parameters $\delta_1 = d_1 c_{E_1}$, with all other parameter values fixed. We can see that this parameter is a bifurcation control parameter, as modifying its value drives the system from bistability (**Fig. S2 (a)** and **(b)**) to monostability (**Fig. S2 (c)**) via a saddle-node bifurcation (Strogatz, 1994). In the bistable regime shown in **Fig. S2 (a)** and **(b)**, the two stable states correspond to the two states of epigenetic regulation: methylated (high steady-state value of $x_{22}(x_{25})$ and low stationary value of $x_{26}(x_{28})$) or acetylated (low steady-state value of $x_{22}(x_{25})$ and high stationary value of $x_{26}(x_{28})$).

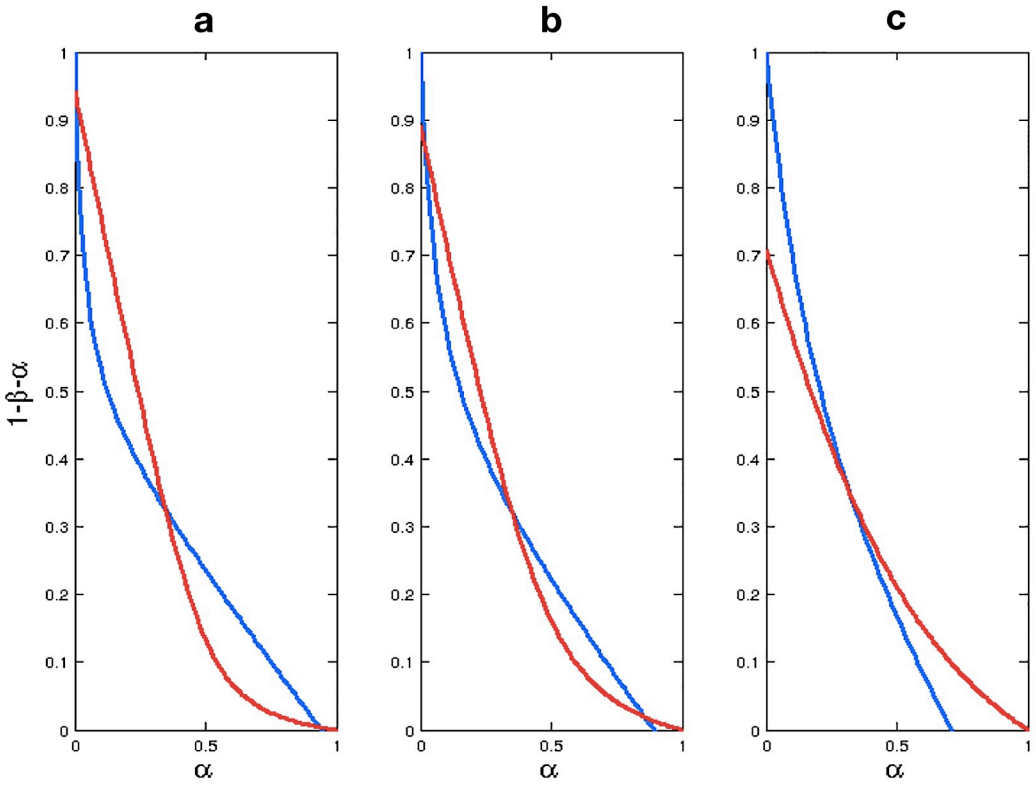

Figure S2. Plots showing the null-clines corresponding to the epigenetic regulation system (40) and (41) for different values of δ_1 . Panel (**a**) corresponds to δ_1 = 0.054, panel (**b**) to δ_1 = 0.026, and panel (**c**) to δ_1 = 0.0054. Other parameter values are taken from **Table E1**.

Our baseline scenario also requires that, in the absence of *OCT4* and *SOX2* induction and 2HG-induced reduction of HDM activity, our system must produce differentiated cells, which requires the epigenetic regulation model of both *LSG1* and *LSG2* to be acetylated so that transcription factors can access their promoters, whereupon differentiation ensues. This requirement is achieved by biasing (reducing) the activity parameter of the corresponding histone deacetylases. **Fig. S3** shows a stochastic simulation for the joint probability density

for the number of methylated and acetylated sites of our stochastic epigenetic regulation model. **Fig. S3** shows the corresponding result for the baseline scenario, which can be interpreted as implying that the time spent by the epigenetic regulatory system in the acetylated state is overwhelmingly longer than the time spent in the methylated state.

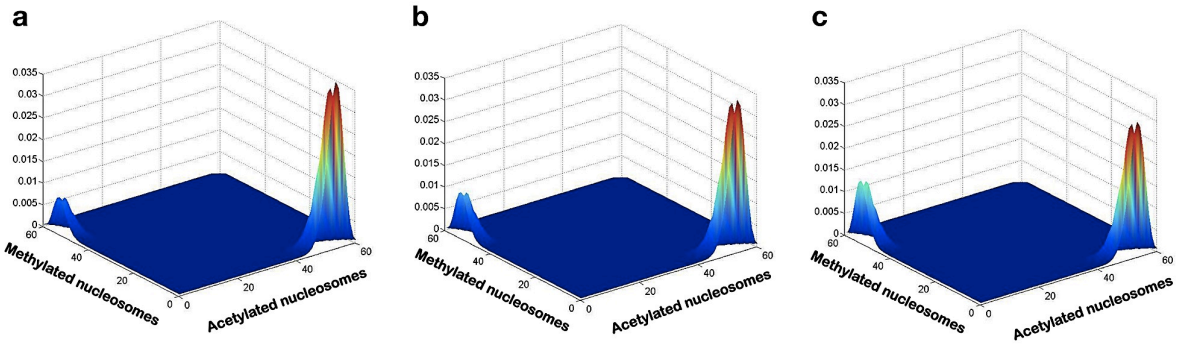

Figure S3. Stochastic simulation results for the probability density of our stochastic model of epigenetic regulation. Panel (**a**) shows a baseline scenario that corresponds to the parameter values given in **Table E1**. Panels (**b**) and (**c**) show two cases of 2HG-induced reduction of HDM activity with respect to the baseline scenario (b: $h_2 = 0.975$ and c: $h_2 = 0.97$).

The parameters corresponding to our baseline scenario are chosen so that (i) the epigenetic regulation system **[40]**-**[41]** and **[43]**-**[44]**, corresponding to *LSG1* and *LSG2*, respectively, are in the bistable regime (see **Fig. S2**), and (ii) the acetylated state is the most stable of the two stable states (see **Fig. S3**). The parameter values compatible with these general properties are given in **Table S7**.

APPENDIX E. Stability analysis of the gene regulatory model in the base-line scenario

Considering the following simplifying assumptions: (i) all the dimer-promoter binding constants are the same, (ii) all the dimer-promoter unbinding constants are the same, (iii) all the gene products are synthesised at the same rate, and (iv) all the proteins are degraded at the same rate, the system of equations **[29]** to **[32]** can be re-written as follows:

$$\frac{dx_1}{d\tau} = p_2 b_1 \frac{x_1 x_3}{1 + a\left(x_1 x_3 + x_5^2 + x_7^2\right)} - c x_1 \qquad \textbf{[E1]}$$

$$\frac{dx_3}{d\tau} = p_4 b_1 \frac{x_1 x_3}{1 + a\left(x_1 x_3 + x_5^2 + x_7^2\right)} - c x_3 \qquad \textbf{[E2]}$$

$$\frac{dx_5}{d\tau} = p_6 b_1 \frac{x_5^2}{1 + a\left(x_1 x_3 + x_5^2 + x_7^2\right)} - c x_5 \qquad \textbf{[E3]}$$

$$\frac{dx_7}{d\tau} = p_8 b_1 \frac{x_7^2}{1 + a\left(x_1 x_3 + x_5^2 + x_7^2\right)} - c x_7 \qquad \textbf{[E4]}$$

where

$$a = \frac{1}{\kappa_{12}} = \frac{\kappa_{13}}{\kappa_{14}} = \frac{\kappa_{15}}{\kappa_{16}} = \frac{\kappa_{17}}{\kappa_{18}} = \frac{\kappa_{19}}{\kappa_{20}} = \frac{\kappa_{21}}{\kappa_{22}} = \frac{\kappa_{23}}{\kappa_{24}} = \frac{\kappa_{25}}{\kappa_{26}} = \frac{\kappa_{27}}{\kappa_{28}} = \frac{\kappa_{29}}{\kappa_{30}} = \frac{\kappa_{31}}{\kappa_{32}} = \frac{\kappa_{33}}{\kappa_{34}} \qquad \textbf{[E5]}$$

$$b_1 = \vartheta_O \frac{\kappa_1}{\kappa_1} = \vartheta_O \kappa_3 \frac{\kappa_{17}}{\kappa_{18}} \qquad \textbf{[E6]}$$

$$b_2 = \vartheta_1 \kappa_5 \frac{\kappa_{25}}{\kappa_{26}} = \vartheta_2 \kappa_7 \frac{\kappa_{31}}{\kappa_{32}} \qquad \textbf{[E7]}$$

$$c = \kappa_2 = \kappa_4 = \kappa_6 = \kappa_8 \qquad \textbf{[E8]}$$

In this appendix, we analyse the conditions for the existence and stability of three fixed points of the form:

$$x_p = (\alpha, \alpha, 0, 0) \qquad \textbf{[E9]}$$

$$x_1 = (0, 0, \beta, 0) \qquad \textbf{[E10]}$$

$$x_2 = (0, 0, 0, \beta) \qquad \textbf{[E11]}$$

where the first, second, third, and fourth components correspond to the steady-state value of *OCT4*, *SOX2*, *LSG1* and *LSG2*, respectively; x_p corresponds to the pluripotency steady state, and x_1 and x_2 correspond to each of the differentiated state states.

We also examine the existence and stability of a fixed point given by:

$$x_U = (\alpha, \alpha, \beta, 0) \qquad \textbf{[E12]}$$

Existence and linear stability of x_p, x_1 *and* x_2. We begin our analysis by examining the properties of x_p. By using the steady-state version of equations **[E1]** to **[E4]** (i.e., $\frac{dx_1}{d\tau} = 0$), we have that, from **[E1]** and **[E2]**, α must satisfy:

$$ca\alpha^2 - p_2 b_1 \alpha + c = 0 \qquad \textbf{[E13]}$$

$$ca\alpha^2 - p_4 b_1 \alpha + c = 0 \qquad \textbf{[E14]}$$

which implies that $p_2 = p_4$ ‡.

‡ If $p_2 \neq p_4$, we have a steady-state $x_p = (\alpha_1, \alpha_2, 0, 0)$, which has the same properties as x_p

The equations **[E3]** and **[E4]** are trivially satisfied. If this restriction on p_2 and p_4 is satisfied, then α is given by:

$$\alpha = \frac{p_2 b_1}{2ac}\left(1 \pm \sqrt{1 - 4\frac{ac^2}{p_2 b_1}}\right) \qquad \textbf{[E15]}$$

According to this equation, for α to be real, the following condition must be satisfied:

$$4\frac{ac^2}{p_2 b_1} \leq 1 \qquad \textbf{[E16]}$$

Provided that **[16]**, the linear stability of x_p is determined by the sign of the eigenvalues of the corresponding Jacobian matrix, J_p, obtained by linearising the right hand side of equations **[E1]** to **[E4]** around x_p, which is given by:

$$J_p = \begin{pmatrix} A_p & 0 & 0 \\ 0 & -c & 0 \\ 0 & 0 & -c \end{pmatrix} \qquad \textbf{[E17]}$$

where A_p is a 2 x 2 matrix corresponding to the linearisation of equations **[E1]** and **[E2]**.

$$A_p = \begin{pmatrix} \frac{p_2 b_1 \alpha}{\left(1 + a\alpha^2\right)^2} - c & \frac{p_2 b_1 \alpha}{\left(1 + a\alpha^2\right)^2} \\ \frac{p_2 b_1 \alpha}{\left(1 + a\alpha^2\right)^2} & \frac{p_2 b_1 \alpha}{\left(1 + a\alpha^2\right)^2} - c \end{pmatrix} \qquad \textbf{[E18]}$$

Given the block structure of J_p, its eigenvalues are the eigenvalues of each block, i.e.:

$$\lambda_1 = \lambda_2 = \lambda_3 = -c \qquad \textbf{[E19]}$$

$$\lambda_4 = 2\frac{p_2 b_1 \alpha}{\left(1 + a\alpha^2\right)^2} - c \qquad \textbf{[E20]}$$

As for x_p to be stable, all the eigenvalues of the Jacobian J_p must be negative, we have a second condition that the system must satisfy:

$$c > 2\frac{p_2 b_2 \alpha}{\left(1 - a\alpha^2\right)^2} \qquad \textbf{[E21]}$$

An analogous analysis regarding the conditions for the existence of x_1 and x_2 leads to the following conditions:

$$4\frac{ac^2}{p_6 b_2} \leq 1 \qquad \textbf{[E22]}$$

$$4\frac{ac^2}{p_8 b_2} \leq 1 \qquad \textbf{[E23]}$$

respectively. Similarly, for them to be stable, the following conditions must hold:

$$c > 2\frac{p_6 b_2 \beta}{\left(1 - a\beta^2\right)^2} \qquad \textbf{[E24]}$$

$$c > 2\frac{p_8 b_2 \beta}{\left(1 - a\beta^2\right)^2} \qquad \textbf{[E25]}$$

The less restrictive pair of existence-stability conditions gives the region of coexistence of the three states as stable steady states. Parameter values compatible with such situations are given in **Table S7**.

Table S7

Parameter	Value	Description	References
T_0	60	Characteristic scale for number of binding sites	[Dodd et al., 2007]
y_0	600	Characteristic scale for number of protein	
h_1	1	Activity of histone methyl transferases	
h_2	1	Activity of histone demethylases	
h_3	1	Activity of histone acetyl transferases	
h_4	0.9	Activity of histone deacetylases	
d_1	0.027	Rate of recruited nucleosome modifications	
d_2	0.003	Rate of unrecruited nucleosome modifications	
d_3	0.425	See **Appendix C**	
c_{E_1}	0.425	See **Appendix C**	
c_{E_1}	$9 \cdot 10^5$	Re-scaled dimer-promoter affinity (See **Appendix E**)	
b_1	5	Re-scaled rate of OCT4 and SOX2 protein production (See **Appendix E**)	

b_2	10	Re-scaled rate of LSG1 and LSG2 protein production (See **Appendix E**)
c	$1.1 \cdot 10^{-6}$	Re-scaled rate of protein degradation (See **Appendix E**)
c_0	1	See **Appendix C**
c_S	1	See **Appendix C**
c_2	1	See **Appendix C**
c_2	1	See **Appendix C**

Parameter values corresponding to the baseline scenario

APPENDIX F. Competition and invasion for clones originated from CSCs *de novo* generated by nuclear reprogramming

We have analysed a mathematical model of competition between two cell populations, i.e., a native, "resident" population sustained by normal stem cells (SCs) and an "invader" population of cancer stem cells (CSCs) *de novo* generated by oncometabolic nuclear reprogramming. We focused on the so-called *neutral scenario.* We assumed that reprogrammed CSCs display the same features as normal SCs, i.e., they possess the same self-renewal and differentiation rates and, crucially, are under the same homeostatic controls than their healthy counterparts. By choosing this setting that corresponds to a base-line case of *least favourable invasion*, we are faced with a situation in which the CSCs are initially under zero-net growth conditions, i.e., identical to that of the native (healthy) cell population. This implies that the early evolution of the invader can be studied in terms of a simple diffusion equation, since its dynamic is essentially dictated by fluctuations due to smallness of the cell population.

Introduction. We herein addressed how significant is the increase of reprogramming rate observed in our proof-of-concept studies with live cells in terms of cancer evolution. In our hands, the number of reprogrammed CSC-like colonies increased by >10 times in the presence of the oncometabolite 2HG. In this appendix we propose a simple mathematical model of cancer evolution in which we demonstrate that the probability of spontaneous clearance of an invader generated by a colony of *de novo* reprogrammed CSCs decreases exponentially with the size of the colony.

Model formulation

Model hypotheses

Our modelling approach is based on a wealth of papers that have approached the problem of regulation of differentiation cascades (Marciniak-Czochra et al., 2009; Pepper et al., 2007; Rodriguez-Brenes et al., 2010; Sánchez-Taltavull and Alarcón, 2014).

(i) We assume that a hierarchical differential cascade maintains each population:

$$\text{Resident: SC} \rightarrow \text{TAC1} \rightarrow \text{TAC2} \cdots \rightarrow \text{MC}$$
$$\text{Invader: CSC} \rightarrow \text{TAC1} \rightarrow \text{TAC2} \cdots \rightarrow \text{MC}$$

SC: stem cell, CSC: cancer stem cell, TAC: transient amplifying cell, MC: mature (fully differentiated) cell.

We assume that the length of the differentiation cascade (i.e. the number of stages between SC or CSC and MC), L, is the same for both populations. SCs and CSCs are the only cell types with the ability for self-renewal whereas TACs are assumed to differentiate upon proliferation.

(ii) Both populations are assumed to compete for a common pool of resources. As far as the model is concerned, this is implemented through a carrying capacity that limits the size of the total population (i.e., resident *plus* invader).

(iii) We consider the most disfavourable situation from the point of view of the invader, i.e. we will assume a neutral scenario in which all the parameter values, e.g. birth rates, death rates, differentiation rates, etc. are set to be the same for both populations. We examine the ability for an invader to take over the resident population as a function of the number of CSCs (equivalently, of the rate of reprogramming of somatic MCs).

(iv) Population dynamics (Pepper et al., 2007, Sánchez-Taltavull and Alarcón, 2014):

(a) SCs and CSCs undergo:

- Asymmetric division at a rate:

$$(1-\epsilon)p_0 e^{-M/K}$$

where $M = M_r + M_i$ with M_r and M_i are the number of mature cells of the resident and invader, respectively. K is the carrying capacity and the probability of SC (CSC) symmetric division. Note that if $M>>K$ (i.e. the mature population is much larger than the carrying capacity) the division rate tends to zero, whereas when $M<<K$ the proliferation rate approaches its maximum value.

- Symmetric self-renewal at a rate:

$$(1 - d_0)\epsilon p_0 e^{-M/K}$$

where d_0 is the probability of symmetric SC (CSC) differentiation.

- Symmetric differentiation at a rate:

$$d_0 \epsilon p_0 e^{-M/K}$$

- Apoptosis at a rate l_0. We will assume that both SCs and CSCs undergo cell death at a very slow rate.

(b) For simplicity and without loss of generality we assume that all TACs differentiate and die at the same rate, regardless of their position in the cascade:

(c) Symmetric differentiation at a constant rate d_1

(d) Apoptosis at a rate λ_1

(e) Mature cells undergo death at a constant rate λ_3

Table S8

Event (Resident population)	Transiton rate	r_k
Asymmetric SC division	$W_{r_1} = (1-\epsilon)p_0 e^{-M/K} X_{r_1}$	$r_{r_1} = (0,+1,0,\ldots,0)$
Symmetric SC self-newal	$W_{r_2} = \epsilon(1-d_0)p_0 e^{-M/K} X_{r_1}$	$r_{r_2} = (+1,0,0,\ldots,0)$
Symmetric SC differentiation	$W_{r_3} = \epsilon d_0 p_0 e^{-M/K} X_{r_1}$	$r_{r_3} = (-1,+2,0,\ldots,0)$
SC apoptosis	$W_{r_4} = \lambda_0 X_{r_1}$	$r_{r_4} = (-1,0,0,\ldots,0)$
Symmetric jth-TAC differentiation	$W_{r_{4+2(j-2)+1}} = d_1 X_{r_j}$	$r_{r_{4+2(j-2)+1}} = (0,0,\ldots,-1,+2,\ldots,0)$
TAC apoptosis	$W_{r_{4+2(j-2)+2}} = \lambda_1 X_{r_j}$	$r_{r_{4+2(j-2)+2}} = (0,0,\ldots,-1,0,\ldots,0)$
MC apoptosis	$W_{r_{4+2(L-3)+3}} = \lambda_3 X_{r_L}$	$r_{r_{4+2(L-3)+3}} = (0,0,0,\ldots,-1)$
Event (Invader population)	Transiton rate	r_k
Asymmetric CSC division	$W_{i_1} = (1-\epsilon)p_0 e^{-M/K} X_{i_1}$	$r_{i_1} = (0,+1,0,\ldots,0)$
Symmetric CSC self-newal	$W_{i_2} = (1-d_0)\epsilon p_0 e^{-M/K} X_{i_1}$	$r_{i_2} = (+1,0,0,\ldots,0)$
Symmetric CSC differentiation	$W_{i_3} = d_0 \epsilon p_0 e^{-M/K} X_{i_1}$	$r_{i_3} = (-1,+2,0,\ldots,0)$
SC apoptosis	$W_{i_4} = \lambda_0 X_{i_1}$	$r_{i_4} = (-1,0,0,\ldots,0)$
Symmetric jth-TAC differentiation	$W_{i_{4+2(j-2)+1}} = d_1 X_{i_j}$	$r_{i_{4+2(j-2)+1}} = (0,0,\ldots,-1,+2,\ldots,0)$
TAC apoptosis	$W_{i_{4+2(j-2)+2}} = \lambda_1 X_{i_j}$	$r_{i_{4+2(j-2)+2}} = (0,0,\ldots,-1,0,\ldots,0)$
MC apoptosis	$W_{i_{4+2(L-3)+3}} = \lambda_3 X_{i_L}$	$r_{i_{4+2(L-3)+3}} = (0,0,0,\ldots,-1)$

Transition rates associated to the stochastic dynamics of the competition between the resident and the invader hierarchical populations. X_{r1} and X_{i1} are the number of SC and CSCs, respectively, X_{rj} and X_{ij}, $j=2, \ldots, L-1$, are the number of TACs of the resident and invader, respectively and X_{rL} and X_{iL} are the number of the mature cells in either population. The total mature population, M, is given by $M=X_{rL}+X_{iL}$.

Stochastic dynamics

The stochastic population dynamics of the system described in the above mentioned section is described in terms of the Master Equation **[1]** (Gardiner, 2009):

$$\frac{\partial P(X,t)}{\partial t} = \sum_{i=1}^{R} \left(W_i(X - r_i) P(X - r_i, t) - W_i(X) P(X,t) \right) \quad \textbf{[F1]}$$

The associated rates, W_i, and stoichiometric vectors, r_i, are given in **Table S8**. X is the $2L$-dimensional state vector whose entries are the numbers of each cellular type in the population.

Setup and initial conditions

We consider a setup or initial condition in which the resident population is let to evolve until it reaches a steady state. This steady state is described (on average) by the mean-field limit of the stochastic dynamics, as shown below. Once the resident steady state has been reached, we evaluate the behaviour of the invader population as a function of the number of *de novo* generated CSCs.

Model analysis

We start by discussing the behaviour of mean-field limit, in particular regarding its steady states. We then proceed to study the diffusion limit of the Master Equation **[1]**, which provides closed form solutions for the clearance probability of the invader.

Mean-field limit

- *Mean-field limit in the absence of invader.* We start by the describing the mean-field limit (Gillespie, 1976) associated to the resident population in the absence of the invader. The Master Equation **[F1]** is then given by the following system of ordinary differential equations:

$$\frac{dx_{r_1}}{dt} = \left(\epsilon(1-d_0)p_0 e^{-x_{r_L}} - \epsilon d_0 p_0 e^{-x_{r_L}} - \lambda_0\right) x_{r_1} \quad \textbf{[F2]}$$

$$\frac{dx_{r_2}}{dt} = 2\epsilon d_0 p_0 e^{-x_{r_L}} x_{r_1} - (d_1+\lambda_1) x_{r_2} \quad \textbf{[F3]}$$

$$\frac{dx_{r_j}}{dt} = 2d_1 x_{r_{j-1}} - (d_1-\lambda_1) x_{r_j},\ j = 3,\ldots,L-1 \quad \textbf{[F4]}$$

$$\frac{dx_{r_L}}{dt} = 2d_1 x_{r_{L-1}} - \lambda_2 x_{r_L} \quad \textbf{[F5]}$$

where $x_{ri}=X_{ri}/K$. Eqs. **[F2]** to **[F5]** have two steady states: the trivial equilibrium $(x_{r1}, x_{r2}, \ldots, x_{rj}, \ldots, x_{rL}) = (0, 0, \ldots, 0, \ldots, 0)$ and the stable positive equilibrium given by:

$$x_{r_1} = \frac{d_1+\lambda_1}{2\epsilon d_0 p_0 e^{-x_{r_L}}} x_{r_2}, \quad \textbf{[F6]}$$

$$x_{r_j} = \frac{d_1+\lambda_1}{2d_1} x_{r_{(j+1)}},\ j = 3,\ldots,L-1, \quad \textbf{[F7]}$$

$$x_{r_L} = -\log\left(\frac{\lambda_0}{\epsilon(1-2d_0)p_0}\right). \quad \textbf{[F8]}$$

The positive equilibrium exists provided that:

$$\frac{\lambda_0}{\epsilon(1-2d_0)p_0} < 1 \text{ and } d_0 < \frac{1}{2}$$

Eq. **[F8]** is obtained by imposing that the net growth rate of the SC population is equal to zero:

$$\epsilon(1-2d_0)p_0 e^{-x_{r_L}} - \lambda_0 = 0.$$

- *Mean-field limit in the presence of the invader.* The presence of the invader substantially changes the structure of the steady states of the model. First, the mean-field equations for the whole system (resident *plus* invader) are:

$$\frac{dx_{r_1}}{dt} = \left(\epsilon(1-d_0)p_0 e^{-(x_{r_L}+x_{i_l})} - \epsilon d_0 p_0 e^{-(x_{r_L}+x_{i_l})} - \lambda_0\right) x_{r_1} \quad \textbf{[F9]}$$

$$\frac{dx_{r_2}}{dt} = 2\epsilon d_0 p_0 e^{-x_{r_L}} x_{r_1} - (d_1+\lambda_1)x_{r_2} \quad \textbf{[F10]}$$

$$\frac{dx_{r_j}}{dt} = 2d_1 x_{r_{j-1}} - (d_1-\lambda_1)x_{r_j},\ j=3,\ldots,L-1 \quad \textbf{[F11]}$$

$$\frac{dx_{r_L}}{dt} = 2d_1 x_{r_{L-1}} - \lambda_2 x_{r_L} \quad \textbf{[F12]}$$

$$\frac{dx_{i_1}}{dt} = \left(\epsilon(1-d_0)p_0 e^{-(x_{r_L}+x_{i_l})} - \epsilon d_0 p_0 e^{-(x_{r_L}+x_{i_l})} - \lambda_0\right) x_{i_1} \quad \textbf{[F13]}$$

$$\frac{dx_{i_2}}{dt} = 2\epsilon d_0 p_0 e^{-(x_{r_L}+x_{i_l})} x_{i_1} - (d_1+\lambda_1)x_{i_2} \quad \textbf{[F14]}$$

$$\frac{dx_{i_j}}{dt} = 2d_1 x_{r_{i-1}} - (d_1-\lambda_1)x_{i_j},\ j=3,\ldots,L-1 \quad \textbf{[F15]}$$

$$\frac{dx_{i_L}}{dt} = 2d_1 x_{i_{L-1}} - \lambda_2 x_{i_L} \quad \textbf{[F16]}$$

where $x_{rl} = Xrl/K$ and $x_{il} = X_{il}/K$.

As in the previous case, Eqs. **[F9]** to **[F16]**, have two steady states: the trivial equilibrium $(x_{r1}, x_{r2}, \ldots, x_{rj}, \ldots, x_{rL}, x_{i1}, x_{i2}, \ldots, x_{ij}, \ldots, x_{iL}) = (0, 0, \ldots, 0, \ldots, 0, 0, 0, \ldots, 0, \ldots, 0)$. The associated positive equilibrium is given by:

$$x_{r_1} = \frac{d_1+\lambda_1}{2\epsilon d_0 p_0 e^{-(x_{r_L}+x_{i_l})}} x_{r_2}, \quad \textbf{[F17]}$$

$$x_{r_j} = \frac{d_1+\lambda_1}{2d_1} x_{r_{(j+1)}},\ j=3,\ldots,L-1, \quad \textbf{[F18]}$$

$$x_{i_1} = \frac{d_1+\lambda_1}{2\epsilon d_0 p_0 e^{-(x_{r_L}+x_{i_l})}} x_{i_2}, \quad \textbf{[F19]}$$

$$x_{i_j} = \frac{d_1+\lambda_1}{2d_1} x_{i_{(j+1)}},\ j=3,\ldots,L-1, \quad \textbf{[F20]}$$

$$x_{r_L} + x_{i_L} = -\log\left(\frac{\lambda_0}{\epsilon(1-2d_0)p_0}\right) \equiv \Omega. \quad \textbf{[F21]}$$

Note that in the presence of the invader, the system does not exhibit a unique positive equilibrium but rather a continuum of equilibria determined by Eq. **[F21]**. Eq. **[F21]** is a restatement of the requirement that the growth rate of the SCs and CSCs is equal to zero. The positive equilibria exist provided that:

$$\frac{\lambda_0}{\epsilon(1-2d_0)p_0} < 1 \text{ and } d_0 < \frac{1}{2}$$

Neutral dynamics: Fokker-Planck equation with demographical noise

We now formulate a diffusion approximation of the stochastic process under the following conditions: Once the resident population has settled down onto its steady state, we introduce a number of *de novo* reprogrammed CSCs and study the behaviour of the invader population generated by the CSCs. The diffusion approximation allows us to find closed form analytical expressions for how the probability of clearance of the invader varies as the number of CSCs changes.

Before proceeding with the formal derivation of the diffusion approximation, an important caveat, which greatly simplifies the analysis, is in order. The scenario we are contemplating, in which a number of CSCs appear in the system (in steady state) as a result of oncometabolic reprogramming of somatic mature cells, implies that both the SC (i.e. the native stem cells of the healthy, resident tissue) and the CSC populations are under conditions of zero net growth rate. Initially, X_{iL}, the number of fully differentiated cells associated to the invader, is $X_{iL}=0$ and X_{iL} is similar to N where $N \equiv \Omega K$, which satisfies the equilibrium condition whereby the growth rate of the CSC population is zero, i.e., the dynamics of the CSC population is critical. Since this condition is initially fulfilled, the whole system continues to evolve under conditions so that Eqs. **[17]** to **[21]** are satisfied at any later time.

Under these conditions, the dynamics of the CSC population is critical with an average total mature population given by Eq. **[21]**. Therefore, its dynamics is entirely dominated by fluctuations. Furthermore, if we assume that K is big enough so that $X_{rL} + X_{iL}$ is similar to N(=cnt.), we can assume that the dynamics of the CSCs is decoupled and can be studied independently.

Diffusion approximation: system size expansion. The systems size expansion is a well-established technique, originally proposed by Kampen et al. (2008), to extract the mean- field limit, i.e., the deterministic behaviour associated to infinite systems where no fluctuations are present, and its first stochastic correction given by the Fokker-Planck equation for the Gaussian fluctuations around the mean-field behaviour (Gardiner, 2006; Kampen et al., 2008). This approximation has been widely used and successfully applied to many different types of problems.

The original approach of Kampen et al. (2008) has been recently critiqued by Di Patti et al (2011), who noted that it breaks down for systems with absorbing states (e.g. extinctions) in the proximity of the absorbing state. They further propose a modification of the basic size expansion that exhibits improved accuracy for systems with absorbing states. The system size expansion is based on the following assumption regarding the stochastic process:

$$X(t) = Nx(t) + N^{\alpha}\xi(t),$$

where N is a measure of system size, $X(t)$ is the mean-field limit, $\xi(t)$ is a stochastic correction to the mean-field. In the original proposal by Kampen et al. (2008) $\alpha = 1/2$, which implies that the size of the effects of noise relative to the size of the systematic (mean-field part) decreases as $N^{-1/2}$ as system size grows. This Ansatz produces a consistent expansion which, at the lowest order, yields a linear-noise (i.e. independent of $\xi(t)$) Fokker-Planck equation (FPE) for the probability density function (PDF) of ξ.

Di Patti et al. (2011) have shown that, in the case in which the stochastic process has an absorbing state, the Van Kampen's Ansatz is no longer consistent. On the contrary, for the system size expansion to be consistent they show that $\alpha = 0$, i.e. the size of the effects of noise is independent of system size. In this case, the Fokker-Planck equation one obtains for the PDF of ξ(t) is no longer a linear-noise equation. On the contrary, one obtains an FPE with a particular type of non-linear (i.e. dependent on the random variable ξ(t)) noise which we refer to as demographic noise. We proceed now to formulate the associated FPE for our system. For the technical details regarding the expansion, we refer the reader to Di Patti et al. (2011).

Assuming that $X_{rL} + X_{iL} \cong N$, we can define a stochastic dynamics for the evolution of the number of CSCs defined by the transition rates:

$$\begin{aligned} W_1(X_{i_1}) &= e^{-\Omega}\epsilon p_0(1-d_0)X_{i_1},\ r_1 = +1, \\ W_2(X_{i_1}) &= e^{-\Omega}\epsilon p_0 d_0 X_{i_1},\ r_2 = -1, \\ W_3(X_{i_1}) &= \lambda_0 X_{i_1},\ r_3 = -1. \end{aligned}$$

We further define $T_{\pm}(z_{iI})$ where $z_{iI} = X_{iI}/N$ as:

$$T_+(z_{i_1}) = e^{-\Omega}\epsilon p_0(1-d_0)z_{i_1}, T_-(z_{i_1}) = (e^{-\Omega}\epsilon p_0 d_0 + \lambda_0)z_{i_1}. \quad \textbf{[F22]}$$

Finally, we expand the quantities $T_{\pm}(z_{iI}) = T_{\pm}(\varphi+N^{\alpha-1}\xi)$ as a power series of $y \equiv N^{\alpha-1}\xi(t)$:

$$T_\pm(\phi+y) = \sum_{k=0} T_\pm^{(k)}(\phi)\frac{y^k}{k!} \quad \textbf{[F23]}$$

With the above definitions, Di Patti et al. (2011) have shown that the Fokker-Planck equation for the PDF of $\xi(t)$, $P(\xi,t)$, is given by:

$$\frac{\partial P}{\partial t} = \left(T_+^{(1)}(0) - T_-^{(1)}(0)\right)\frac{\partial}{\partial \xi}(\xi P) + \frac{1}{2}\left(T_+^{(1)}(0) + T_-^{(1)}(0)\right)\frac{\partial^2}{\partial \xi^2}(\xi P). \quad \textbf{[F24]}$$

In our case:

$$T_+^{(1)}(0) + T_-^{(1)}(0) = e^{-\Omega}\epsilon p_0 + \lambda_0,$$

see Eq. **[F21]**, and

$$T_+^{(1)}(0) + T_-^{(1)}(0) = e^{-\Omega}\epsilon p_0 + \lambda_0,$$

and, therefore, Eq. **[F24]** reads:

$$\frac{\partial P}{\partial t} = \frac{D}{2}\frac{\partial^2}{\partial \xi^2}(\xi P). \qquad \textbf{[F25]}$$

where $D \equiv e^{-\Omega} p_0 + \lambda_0$. Eq. **[F25]** is the diffusion approximation for the process of neutral dynamics of the CSC population.

Survival probability of the CSC population: backward Kolmogorov equation. In order to study the survival probability of the CSC population, rather than directly using the FPE Eq. **[F25]**, it is more convenient to use an equivalent description, the so-called Kolmogorov backward equation (KBE) (Demetrius et al., 2009; Gardiner, 2009). Mathematically speaking, the KBE is the adjoint equation of the FPE (also known as the Kolmogorov forward equation). The KBE associated to the Fokker-Planck equation Eq. **[25]** is given by (Demetrius et al., 2009 and Gardiner, 2009):

$$\frac{\partial \Psi}{\partial t} = \frac{D}{2} q \frac{\partial^2 \Psi}{\partial q^2}. \qquad \textbf{[F26]}$$

with natural boundary conditions $\Psi(q=0,t)=0$ and $\Psi(q=\infty,t)=1$. The associated initial condition is $\Psi(q,t=0)=1$ for positive q. With these boundary conditions, the solution of the KBE can be interpreted as the probability of survival of a CSC population of initial size q at time t. The associated clearance probability at time t, $P_C(q, t)$, is therefore given by $P_C(q,t)=1-\Psi(q,t)$.

It is possible to obtain a closed form, analytical solution for Eq. **[F26]** by considering its similarity structure (Ockendon et al., 2003). It is immediate to verify that, if $\Psi(q, t)$ is a solution of Eq. **[F26]**, so is $\Psi(\mu q,\mu t)$ where μ is an arbitrary constant. Therefore, for any given value of t, we can set $\mu=t^{-1}$, so that $\Psi(q,t)=F(q/t)$ for some function F to be determined from Eq. **[F26]**. By writing $\eta=q/t$, Eq. **[F26]** can be re-written as:

$$\frac{D}{2}\frac{d^2 F}{d\eta^2} + \frac{dF}{d\eta} = 0 \qquad \textbf{[F27]}$$

with boundary conditions $F(\eta=0)=0$ and $F(\eta=\infty)=1$. The solution is therefore given by:

$$\Psi(q,t) = F(q/t) = 1 - P_C(q,t) = 1 - (P_1(t))^q = 1 - e^{-\frac{2}{D}\frac{q}{t}} \qquad \textbf{[F28]}$$

where $P_1(t)$ is the probability of clearance of a single CSC at time t. The clearance probability is therefore given by $P_C(q,t)=(P_1(t))^q$. This result implies that the probability of spontaneous clearance of a population generated by a colony of reprogrammed CSCs decreases exponentially as the size of the colony, q, increases. This implies that with a 10 to 20-fold increase in nuclear reprogramming frequency, the chances of clearance of the population generated by the oncometabolically *de novo* reprogrammed CSCs decreases by many orders of magnitude.

In summary, we are able to find an analytical solution for spontaneous clearance probability of the CSC population as a function of the size of the *de novo* reprogrammed CSC pool, q, at time t, $P_C(q,t)=(P_1(t))^q$, where $P_1(t)<1$ is the probability of clearance at time t of a single

CSC. Therefore, from the point of view of cancer evolution, an apparently inefficient 10 to 20-fold increase in the reprogramming frequency is highly significant in terms of the prolonged survival of the initial population generated by the *de novo* reprogrammed CSCs.

Supplemental references

Ablowitz, M. J., Fokas, A. S. *Complex variables. Introduction and applications.* Cambridge University Press, Cambridge, UK. 2003.

Alarcón, T. Stochastic quasi-steady state approximations for asymptotic solutions of the chemical master equation. J. Chem. Phys. 2014;140:184109.

Assaf, M., Meerson, B., Sasorov, P. V. Large fluctuations in stochastic population dynamics: momentum space calculations. J. Stat. Mech. 2010; P07018.

Cinquin, O., Demongeot, J. High-dimensional switches and the modelling of cellular differentiation. J. Theor. Biol. 2005; 233:391-411.

Cinquin, O., Page, K. M. Generalized, switch-like competitive heterodimerization networks. Bull Math. Biol. 2007; 69:483-494.

Demetrius, L., Gundlach, V. M., Ochs, G. Invasion exponents in biological networks. Physica A. 2009; 388: 651-672.

Dickman, R., Vidigal, R. Braz. J. Phys. Path Integrals and Perturbation Theory for Stochastic Processes. 2003; 33:73-93.

Dykman, M. I., Horita, T., Ross, J. Statistical distribution and stochastic resonance in a periodically driven chemical system. J. Chem. Phys. 1995; 103:966-972.

Elgart, V., Kamenev, A. Rare event statistics in reaction-diffusion systems. Phys. Rev. E. Stat. Nonlin. Soft. Matter. Phys. 2004; 70:041106.

Feynman, R. P., Hibbs, A. R. *Quantum Mechanics and Path Integrals*, McGraw Hill: 1965 (ISBN 0-07-020650-3), Dover Publications: 2010.

Gardiner, C. W. *Stochatic methods*. Springer-Verlag, Berlin, Germany. 2009

Gillespie, D. T. A General Method for Numerically Simulating the Stochastic Time Evolution of Coupled Chemical Reactions. J. Comp. Phys. 1976; 22:403-434.

Grimmett, G. R., Stirzaker, D. R. *Probability and random processes*. 2nd ed Oxford University Press. 1992.

Kampen, N. G. V. *Stochastic processes in Physics and Chemistry*. Elsevier, The Netherlands. 2007.

Keener, J., Sneyd, J. *Mathematical physiology*. Springer-Verlag, New York, NY, USA. 1998.

Kubo, R., Matsuo, K., Kitahara, K. Fluctuation and Relaxation of Macrovariables. J. Stat. Phys. 1973; 9:51-96.

MacArthur, B. D., Lemischka, I. R. Statistical mechanics of pluripotency. Cell. 2013; 154: 484-489.

MacArthur, B. D., Please, C. P., Oreffo, R. O. Stochasticity and the molecular mechanisms of induced pluripotency. PLoS One. 2008; 3:e3086.

Marciniak-Czochra, A., Stiehl, T., Ho, A. D., Jäger, W., Wagner, W. Modeling of asymmetric cell division in hematopoietic stem cells--regulation of self-renewal is essential for efficient repopulation. Stem Cells Dev. 2009;18:377-385.

Murray, J. D. *Asymptotic analysis.* Springer-Verlag, New York, NY, USA. 1984.

Di Patti, F., Azaele, S., Banavar, J. R., Maritan, A. System size expansion for systems with an absorbing state. Phys. Rev. E Stat. Nonlin. Soft Matter Phys. 2011; 83:010102.

Pepper, J. W., Sprouffske, K., Maley, C. C. Animal cell differentiation patterns suppress somatic evolution. PLoS Comput. Biol. 2007; 3:e250.

Rodriguez-Brenes, I. A., Wodarz, D., Komarova, N. L. Minimizing the risk of cancer: tissue architecture and cellular replication limits. J. R. Soc. Interface. 2013; 10:20130410.

Sánchez-Taltavull, D., Alarcón, T. Robustness of differentiation cascades with symmetric stem cell division. J. R. Soc. Interface. 2014; 11:20140264.

Sakurai, J. J. *Modern quantum mechanics* (Addison-Wesley, New York, USA) 1994.

Strogatz, S. H. *Non-linear dynamics and chaos.* Perseus Books, Reading, Mass. USA. 1994.

Takahashi, K., Tanabe, K., Ohnuki, M., Narita, M., Ichisaka, T., Tomoda, K., Yamanaka, S. Induction of pluripotent stem cells from adult human fibroblasts by defined factors. Cell. 2007; 131:861-872.

Takahashi, K., Yamanaka, S. Induction of pluripotent stem cells from mouse embryonic and adult fibroblast cultures by defined factors. Cell. 2006; 126:663-676.

Täuber, U. C., Howard, M., Vollmayr-Lee, B. P. Applications of field-theoretic renormalization group methods to reaction-diffusion problems. J. Phys. A: Math. Gen. 2005; 38:R79-R131.

Traulsen, A., Lenaerts, T., Pacheco, J. M., Dingli, D. On the dynamics of neutral mutations in a mathematical model for a homogeneous stem cell population. J. R. Soc. Interface. 2012; 10:20120810.